# Papers

## Algorithm for the remote sensing of the Baltic ecosystem (DESAMBEM). Part 1: Mathematical apparatus*

OCEANOLOGIA, 50 (4), 2008.
pp. 451–508.



**KEYWORDS**
Remote sensing
Marine ecosystem monitoring
Chlorophyll algorithm
Temperature algorithm
Primary production algorithm
Light-photosynthesis model

Bogdan Woźniak[1,3,⋆]
Adam Krężel[2]
Mirosław Darecki[1]
Sławomir B. Woźniak[1]
Roman Majchrowski[3]
Mirosława Ostrowska[1]
Łukasz Kozłowski[2]
Dariusz Ficek[3]
Jerzy Olszewski[1]
Jerzy Dera[1]

[1] Institute of Oceanology, Polish Academy of Sciences,
Powstańców Warszawy 55, PL–81–712 Sopot, Poland

⋆corresponding author, e-mail: wozniak@iopan.gda.pl

[2] Institute of Oceanography, University of Gdańsk,
al. Marszałka Piłsudskiego 46, PL–81–378 Gdynia, Poland

[3] Institute of Physics, Pomeranian Academy,
Arciszewskiego 22B, PL–76–200 Słupsk, Poland

Received 29 April 2008, revised 9 September 2008, accepted 16 October 2008.

* This paper was produced within the framework of the project commissioned by the Polish Committee for Scientific Research – *DEvelopment of a SAtellite Method for Baltic Ecosystem Monitoring – DESAMBEM* (project No. PBZ-KBN 056/P04/2001). On completion of the project, the participating institutes (Institute of Oceanology, Polish Academy of Sciences; Institute of Oceanography, University of Gdańsk; Institute of Physics, Pomeranian Academy, Słupsk) signed an agreement to set up a scientific network known as the *Inter-Institute Group for Satellite Observations of the Marine Environment* (*Międzyinstytutowy Zespół Satelitarnych Obserwacji Środowiska Morskiego*), the aim of which is to undertake further work in this field of research.

**Abstract**

This article is the first of two papers on the remote sensing methods of monitoring the Baltic ecosystem, developed by our team. Earlier, we had produced a series of detailed mathematical models and statistical regularities describing the transport of solar radiation in the atmosphere-sea system, the absorption of this radiation in the water and its utilisation in a variety of processes, most importantly in the photosynthesis occurring in phytoplankton cells, as a source of energy for the functioning of marine ecosystems. The comprehensive DESAMBEM algorithm, presented in this paper, is a synthesis of these models and regularities. This algorithm enables the abiotic properties of the environment as well as the state and the functioning of the Baltic ecosystem to be assessed on the basis of available satellite data. It can be used to determine a good number of these properties: the sea surface temperature, the natural irradiance of the sea surface, the spectral and spatial distributions of solar radiation energy in the water, the surface concentrations and vertical distributions of chlorophyll *a* and other phytoplankton pigments in this sea, the radiation energy absorbed by phytoplankton, the quantum efficiency of photosynthesis and the primary production of organic matter. On the basis of these directly determined properties, other characteristics of processes taking place in the Baltic ecosystem can be estimated indirectly.

Part 1 of this series of articles deals with the detailed mathematical apparatus of the DESAMBEM algorithm. Part 2 will discuss its practical applicability in the satellite monitoring of the sea and will provide an assessment of the accuracy of such remote sensing methods in the monitoring of the Baltic ecosystem (see Darecki et al. 2008 – this issue).

## 1. Introduction

The numerous threats to the Earth's environment, as well as the current frequency of natural disasters brought about by environmental changes, have persuaded specialists to undertake a radical intensification of ecological research and forecasts at both regional and global scales. The processes taking place in the vast marine ecosystems play a key part in these changes, in particular, the assimilation of carbon, the release of oxygen and the production of organic matter by algae (Steemann Nielsen 1975, Falkowski & Raven 2007). The photosynthetic production of algae is the first link in the food chain of marine organisms and is also a significant source of energy for terrestrial ecosystems (Lieth & Whittaker 1975, Falkowski & Knoll (eds.) 2007). Moreover, by affecting the content of oxygen and carbon dioxide in the atmosphere, marine photosynthesis is one of the main factors governing the state of the greenhouse effect and the Earth's climate (Glantz (ed.) 1988, Trenberth (ed.) 1992). These facts are sufficient justification for the need to monitor the marine environment on a continuous basis. Such monitoring using traditional ship-borne methods is, however, extremely costly, not very effective, and does not satisfy

current environmental monitoring criteria. Hence, the last thirty years has seen more and more attempts to utilise the far less expensive and more effective remote sensing methods with the aid of the scanning radiometers installed on board various of the Earth's artificial satellites, e.g. CZCS[1] on the Nimbus 7 satellite, SeaWiFS[2] on OrbView 2, OCTS[3] on ADEOS, MODIS[4] on the Terra and Aqua satellites, and MERIS[5] on Envisat. These methods are based on recording and utilising the spectral characteristics of the light emerging from the waters of oceans, seas and lakes. The recorded colour of the light leaving a basin is compared with the colour of the light entering it. Numerous algorithms have already been developed enabling various parameters describing the state of aquatic basins to be defined on the basis of these spectral light characteristics. These parameters characterise, in turn, the physical, chemical, biological and other processes taking place in those basins (see the monographs by Gordon & Morel 1983, Sathyendranath et al. 2000, Arst 2003). Crucial among these processes is the inflow of solar radiation, its absorption in the aquatic medium and its utilisation in photosynthesis: this process governs the extent to which the marine biocoenosis is supplied with energy and hence governs the functioning of marine ecosystems. Nevertheless, the algorithms already developed and used to determine the ecologically important properties of water basins rely on the recording of the sea's colour, and are applicable to or yield good estimates for areas of clean oceanic waters classified as case 1 waters (Morel & Prieur 1977). Such algorithms are used mainly to estimate resources of chlorophyll (see e.g. Gordon et al. 1988, Sathyendranath et al. 1994, 2001, IOCCG 2007) and to monitor primary production in the ocean (e.g. Platt et al. 1988, 1995, Sathyendranath et al. 1989, Platt & Sathyendranath 1993a,b, Antoine et al. 1996, Antoine & Morel 1996, Campbell et al. 2002, Ficek et al. 2003, Woźniak et al. 2003, Carr et al. 2006). In such case 1 waters, the great majority of admixtures modifying the light field are of autogenic origin, that is, they result from the functioning of the local ecosystem, which is dependent on the photosynthesis of phytoplankton. In consequence, the sea colour in case 1 waters reflects their chlorophyll content, which is an index of their phytoplankton content, their trophicity and other ecological

[1]Coastal Zone Colour Scanner

[2]Sea-viewing Wide Field-of-view Sensor

[3]Ocean Colour and Temperature Scanner

[4]MODerate resolution Imaging Spectroradiometer

[5]MEdium Resolution Imaging Spectrometer

characteristics. This considerably simplifies the construction of algorithms for estimating the ecological properties of these basins by means of remote sensing methods.

Now, where the waters of the coastal zones of oceans, enclosed seas like the Baltic, and closed basins like lakes and rivers are concerned, the construction of such algorithms is a more complicated and difficult undertaking. Apart from chlorophyll and other products of the local ecosystem, the waters of such basins contain many allogenic substances, which have complex optical properties (Jonasz & Fourier 2007, Woźniak & Dera 2007) and modify the colour of the basin in a manner characteristic of the region in question. The colour of such waters – referred to as case 2 waters – recorded by a satellite is therefore not a direct reflection of the chlorophyll concentration. To take this fact into account requires the construction of a far more complicated algorithm, which is adapted to the characteristics of the waters in the region under scrutiny (Sathyendranath et al. 2000, Darecki et al. 2003).

For the Baltic Sea, the Institute of Oceanology PAS, Sopot, in conjunction with the University of Gdańsk's Institute of Oceanography, the Institute of Physics of the Pomeranian Academy, Słupsk, and the Marine Fisheries Institute, Gdynia, carried out in 2001–05 an appropriate research project entitled *Development of a Satellite Method for Baltic Ecosystem Monitoring* (DESAMBEM) (project No. PBZ-KBN 056/P04/2001 commissioned by the Polish Committee for Scientific Research). Although this project has been completed, the above-mentioned institutions are jointly continuing research into this problem. The aim of these studies is to improve the scientific foundations and methods of utilising satellite images for monitoring the Baltic as an enclosed sea, whose biological productivity is high in comparison with the open basins of oceans and which is particularly vulnerable to the effects of economic development. We considered the continuation of these studies to be justified in the light of the ever greater availability of satellite data, which allow large water bodies to be monitored. Moreover, the digital recording of the light emerging from the sea in many different intervals of the electromagnetic spectrum makes it possible to obtain a very wide range of information on the physical, chemical and biological properties of sea waters and also on the processes occurring in them. Armed with this information, one is then in a position to diagnose the states of marine basins, and to make predictions about their transformations and their reactions to different forms of human activities.

During our earlier joint researches we developed a series of detailed mathematical models and statistical relationships describing different properties of the Baltic. These models describe the transfer of solar radiation

in the atmosphere-sea system, the absorption of this radiation in the water and its utilisation in the process of marine photosynthesis in the Baltic. These several models were described in a number of articles, which will be cited in Chapter 2. The synthesis of these models has enabled us, among other things, to develop the DESAMBEM algorithm discussed in the present paper. This algorithm permits the definition of a series of important biotic and abiotic characteristics of the Baltic Sea, as well as the state and functioning of its ecosystem, on the basis of available satellite data. The following properties may be mentioned here: sea surface temperature, surface currents and upwelling events, the extent to which riverine waters penetrate the Baltic, water transparency, Photosynthetically Available Radiation (PAR), the concentration of chlorophylls and other pigments in the water, the efficiency of photosynthesis and the primary production of organic matter, and some other magnitudes characterising the state and functioning of the ecosystem. All these properties can be supplied in the form of spatial distribution maps.

The aim of these two articles (Parts 1 and 2) is to present this algorithm and to assess its usefulness in practical studies of the Baltic ecosystem. In the present paper (Part 1) we describe the algorithm in detail with the aid of diagrams of its component parts and present its complete mathematical apparatus. This description can then be used to estimate the above-mentioned properties of the Baltic ecosystem on the basis of input data obtained from optical signals recorded by satellite sensors, among others, SeaWiFS, MODIS, AVHRR[6] (the last one on the Tiros N/NOAA satellites) and SEVIRI[7] (on the Meteosat satellite). Owing to the complexity of the entire algorithm, this presentation will be restricted to only a formal mathematical description; the detailed interpretation of the physical aspects of the models and statistical regularities underpinning this mathematical apparatus can be found in the description of these models published in our earlier papers (see Chapter 2).

The analysis of the practical usefulness of this algorithm in Baltic studies, based on its validation and an assessment of the errors of the estimated parameters following their empirical verification, will be presented in Part 2 of the series (see Darecki et al. 2008 – this issue).

The principal abbreviations and symbols used in Parts 1 and 2 of this series will be found in Annex VI.

[6]Advanced Very High Resolution Radiometer

[7]Spinning Enhanced Visible and Infra Red Imager

## 2. General outline and block diagrams of the DESAMBEM algorithm

This algorithm makes use of separate mathematical models (physical, or founded on statistical regularities) as the basis for estimating various properties and parameters of the Baltic ecosystem. Most of the models are ones that we ourselves developed, but some we have gleaned from the literature. In a very general way we discussed the scheme of such an algorithm in Woźniak et al. (2004). There we presented a simplified block diagram of the algorithm (shown here in Figure 1). The diagram consists of three sections:

- **Input data** – the parameters describing the state of the atmosphere-sea system, which are essential for calculations and estimates: **Block D.1** – radiometric data performed by satellite sensors in the VIS, near-IR ($IR_1$) and thermal-IR ($IR_2$) ranges; **Block D.2** – further data on the state of the environment routinely available from the hydrological and meteorological services, or generated by operational meteorological models, e.g. atmospheric pressure, air humidity, wind speed and wind direction.
- **Model formulae** – mathematical models describing the links between: **Block M.1** – directly-measured satellite data and selected hydrological and meteorological parameters of the atmosphere-sea system; **Block M.2** – parameters of the state of the atmosphere, its transmittance, and its other optical properties; **Block M.3** – various hydrometeorological parameters, and the state and optical properties of the sea surface; **Block M.4** – spectral values of the reflectance or albedo of the sea, and concentrations of chlorophyll *a* and the other principal components of surface sea water; **Block M.5** – the concentration of chlorophyll *a* at various depths, as well as diverse optical properties of sea water and parameters of the underwater irradiance field; **Block M.6** the concentrations of accessory pigments at various depths and coefficients of light absorption by algae; **Block M.7** – the quantum yield of photosynthesis and primary production in the sea as function of the underwater irradiance, temperature and light absorption by algae, as well as biotic and abiotic factors.
- **Calculations** – the abiotic and biotic parameters of the atmosphere-sea system, determined from the **Input data** with the aid of the **Model formulae**. The details of these estimated parameters are given in Figure 1 (**Blocks C.1** to **C.8**).

The diagram in Figure 1 usefully illustrates the range of calculations covered by the DESAMBEM algorithm, but it is not sufficiently detailed

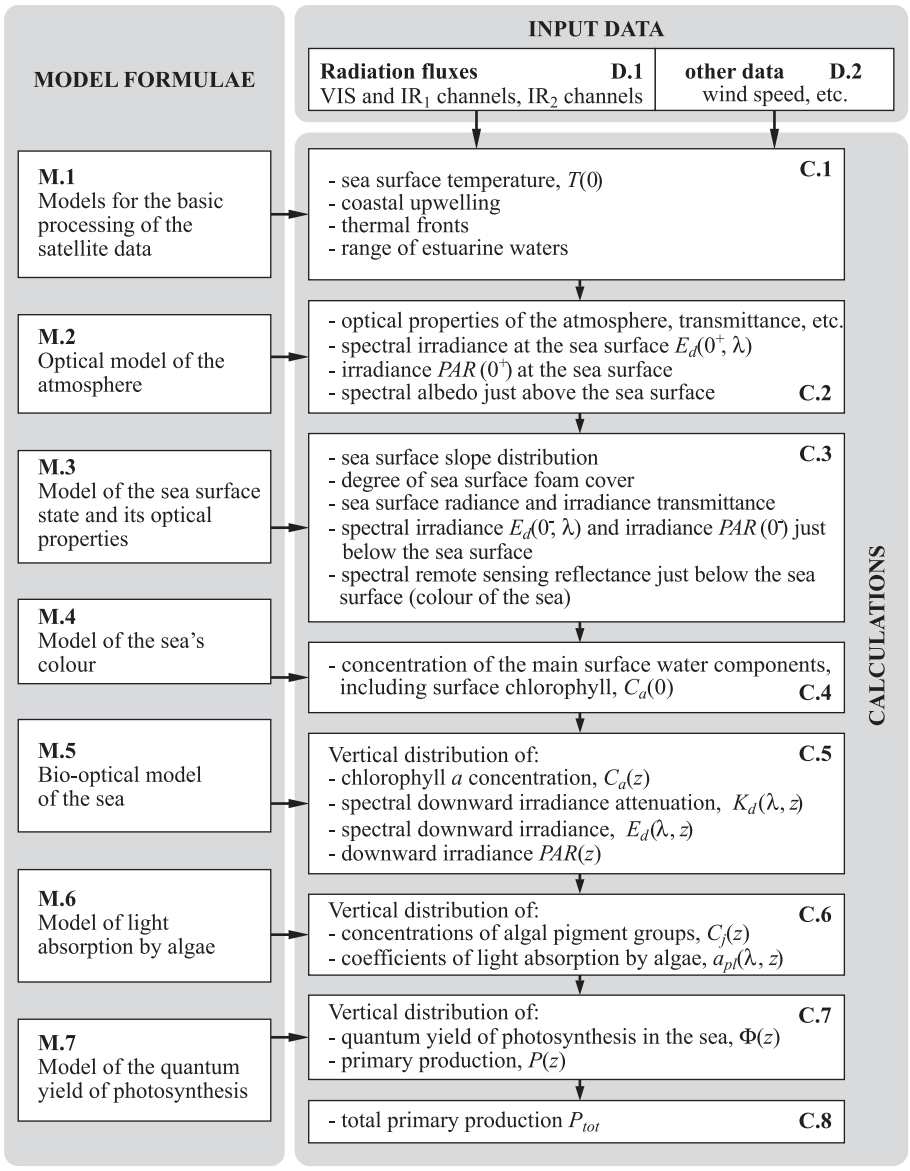


**Figure 1.** Block diagram of the DESAMBEM algorithm (after Woźniak et al. 2004)

to present its complete mathematical apparatus. In order to make such a detailed presentation of all the calculation stages, it is convenient to break this diagram up into five diagrams of subalgorithms covering narrower groups of models utilised in the calculations. These are:

I Subalgorithm for estimating the irradiance at the Baltic Sea surface;

II Subalgorithm for estimating the Baltic Sea surface temperature;

III Subalgorithm for estimating the chlorophyll *a* concentration in the Baltic Sea surface layer;

IV Subalgorithm for calculating the daily dose of PAR transmitted across a wind-blown sea surface;

V Subalgorithm for estimating the underwater optical and bio-optical features and photosynthetic primary production in the Baltic Sea.

Subalgorithms I, II and III are independent of each other and are designed to determine selected properties of the atmosphere-sea system (in this case, the irradiance conditions, temperature and chlorophyll *a* concentration at the sea surface) on the basis of remote-sensing data. Subalgorithms IV and V, however, are interdependent; they are linked with the earlier ones in that they cover the consecutive stages of the calculations in which the parameters calculated in the previous subalgorithm become the input data for the subsequent one. And so the first of these latter two algorithms (here, number IV), enables the determination of the irradiance conditions just beneath the sea surface on the basis of the irradiance conditions just above it, which are the result of the calculations contained in subalgorithm I. Subalgorithm V is the most complicated one, covering as it does a plethora of phenomena occurring in the sea: it enables the determination of numerous bio-optical parameters (from the underwater light fields and radiant energy absorbed in the water to the phytoplankton light absorption capacity, distributions of phytoplankton pigment concentrations and the primary production of organic matter) on the basis of three sets of input data, which result from the calculations of previous subalgorithms, i.e. the irradiance penetrating the water surface (calculated according to subalgorithm IV), the surface concentration of chlorophyll *a* (calculated using subalgorithm III) and the sea surface temperature (determined with subalgorithm II). In this way the above five component subalgorithms combine to form the comprehensive DESAMBEM algorithm for estimating various parameters of the ecosystem on the basis of satellite information.

Block diagrams of these component subalgorithms will be presented (see Figures 2 to 6) and discussed. All the diagrams have been constructed in accordance with analogous logic as a general scheme of the entire DESAMBEM algorithm (Figure 1), that is, they contain three sections: Input data, Model formulae and Calculations. Annexes I, II, III, IV and V provide the complete mathematical apparatus compatible with the block diagram of each subalgorithm.

### 2.1. Subalgorithm for estimating the irradiance at the Baltic Sea surface

The key to this estimation is the simplified block diagram shown in Figure 2. It consists of three sections, which are discussed below.

**Section A** – **the Input data** essential for the calculations include:

- $DOY$, $GMT$, $\lambda_g$, $\varphi_g$ (block 1) – the respective spatio-temporal parameters of the point at sea: the day number of the year, Greenwich Mean Time, longitude, latitude;
- $e$, $p$, $T$ (block 2) – meteorological data, i.e. water vapour pressure, atmospheric pressure, and air temperature above the sea surface respectively;
- $\tau_a$, $L_u$ (block 3) – satellite-derived aerosol optical thickness of the atmosphere (from AVHRR data) and radiance in the HRV channel of SEVIRI.

These meteorological input data can be obtained directly, by measurement at a given position at sea from on board ship, or indirectly, as is usually the case, from the results of meteorological modelling. Here we have used data generated by the ICM[8] model. As far as satellite-derived data are concerned, AVHRR data (spectral channels 0.58–0.68 $\mu$m and 0.72 –1.00 $\mu$m) and SEVIRI (0.6–0.9 $\mu$m) are used.

**Section B** – contains the set of **Model formulae**, either gleaned from the literature or resulting from the modelling carried out by the authors of this paper (see the references cited below). In detail, they are:

- (block 4) – Sun-Earth geometry formulae (after Spencer 1971; see also Krężel 1997), enabling the calculation firstly of the solar zenith angle $\theta$ for a selected position at sea defined by the geographical coordinates $\lambda_g$ and $\varphi_g$ within a selected time-frame defined by the day number of the year $DOY$ and the $GMT$, and secondly, the ratio of the mean to actual Sun-Earth distance $\beta$ dependent on the number $DOY$;
- (block 5) – the solar radiation transmission in the cloudless atmosphere model, described in detail by Krężel (1997) and developed on the basis of data and information contained in e.g. Reitan (1960), Kasten (1966), Leckner (1978), Kneizys et al. (1980), Bird & Riordan (1986) and Gregg & Carder (1990). The formula resulting from this model describes the link between the coefficient of solar radiation

[8]Interdisciplinary Centre for Mathematical and Computational Modelling, Warsaw University – http://www.icm.edu.pl/eng/

transmission through a cloudless atmosphere $T^0$ on the basis of known meteorological data ($e$, $p$, $T$), as well as other meteorological and optical properties of the atmosphere, which are assumed to be fixed;

– (block 6) – the cloud transmission model presented in an earlier paper (Krężel et al. 2008). The formula emerging from this model describes the relationship between the coefficient of light transmission for all clouds $T^r$, the position of the Sun $\theta_\otimes$ and the satellite-derived coefficient of cloudiness $c_T$.

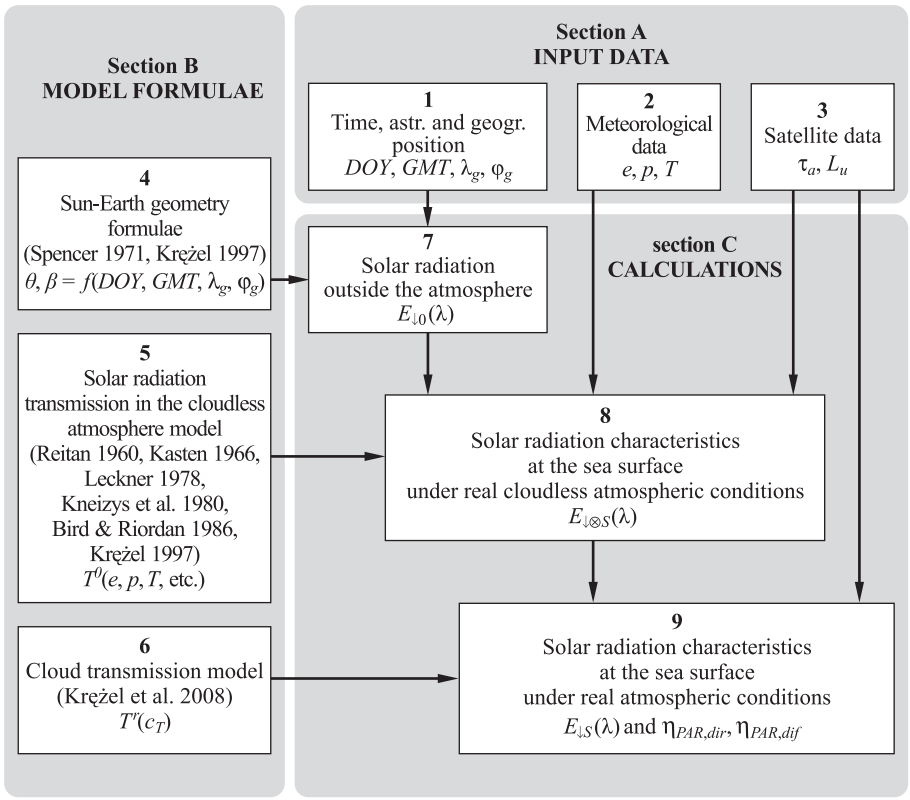


**Figure 2.** Block diagram of the subalgorithm for estimating the irradiance at the Baltic Sea surface (for the mathematical apparatus of this algorithm, see Annex I)

**Section C – Calculations** utilising the input data (blocks 1–3) and the model formulae described above (blocks 4–6) the following characteristics of solar light energy are calculated in turn on the basis of well-known formal relationships in optics: the solar spectral irradiance outside the atmosphere $E_{\downarrow 0}(\lambda)$ (block 7), the solar spectral irradiance at the sea surface under real cloudless atmospheric conditions $E_{\downarrow\otimes S}(\lambda)$ (block 8), and the solar

spectral irradiance at the sea surface under real atmospheric conditions $E_{\downarrow S}(\lambda)$ (block 9). These properties of solar irradiance refer to instantaneous values of spectral energy densities, expressed in units of power. On the other hand, the corresponding doses of these energies in finite intervals of time (e.g. the daily irradiation: direct $\eta_{PAR,\,dir}(0^+)$ and diffuse $\eta_{PAR,\,dif}(0^+)$) and with respect to total but not spectral irradiances (e.g. in the PAR spectral interval, i.e. 400–700 nm), necessary in further calculations of the energy characteristics of light fields in the sea, which in turn are essential for estimating the daily primary production (see Chapter 2.5), can be obtained by appropriately integrating these instantaneous spectral energy densities over time and/or over the solar radiation wavelength.

The complete mathematical apparatus for this subalgorithm for determining the surface irradiance of the Baltic Sea is given in Annex I.

## 2.2. Subalgorithm for estimating the Baltic Sea surface temperature

Figure 3 shows a block diagram of this subalgorithm; it contains the three sections presented below.

**Section A** – **Input data** essential for the calculations include:

- $GMT$, $\varphi_g$, $\lambda_g$ (block 1) – temporal and spatial parameters, i.e. Greenwich Mean Time, latitude and longitude, respectively;
- $L_u(\lambda_1)$, $L_u(\lambda_2)$ (block 2) – satellite derived data, i.e. the radiance in AVHRR channels 4 (10.3–11.3 $\mu$m) and 5 (11.5–12.5 $\mu$m), respectively.

**Section B** – contains the set of **Model formulae** gleaned from the literature, or emerging from our own modelling procedures (see the references cited below). In detail, they are:

- (block 3) satellite positioning formulae and the procedures (after Kowalewski & Krężel 2004, NOAA KLM 2005) enabling the geometric correction of the image and the precise geographical location (latitude and longitude $\varphi_g$ and $\lambda_g$) of each pixel;
- (block 4) – formulae for the instrumental correction and definition of the brightness temperature in AVHRR channels 4 and 5 (NOAA KLM 2005);
- (block 5) – formulae for defining the sea surface temperature on the basis of AVHRR data (see Krężel et al. 2005).

**Section C** – **Calculations** using the input data (blocks 1–2) and the model formulae (blocks 3–5) the following parameters are calculated in turn: sea

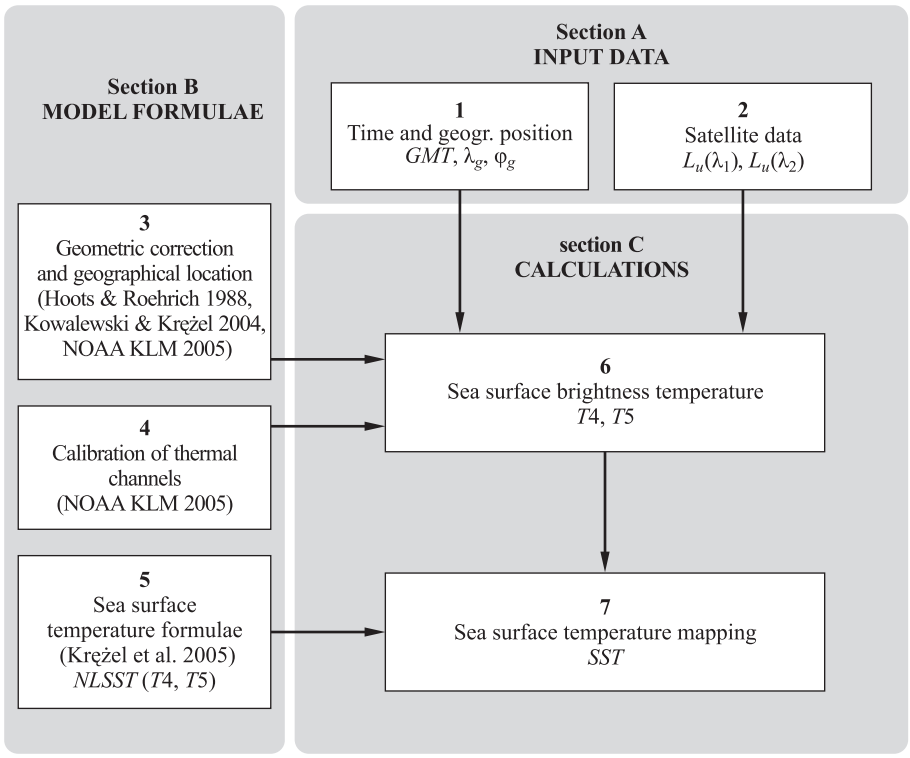


**Figure 3.** Block diagram of the subalgorithm for estimating the Baltic Sea surface temperature (for the mathematical apparatus of this algorithm, see Annex II)

surface brightness temperature in AVHRR channels 4 and 5 (block 6), and then the sea surface temperature (block 7).

The detailed mathematical apparatus of this subalgorithm for determining the surface temperature of the Baltic Sea is given in Annex II.

### 2.3. Subalgorithm for estimating the chlorophyll *a* concentration in the Baltic Sea surface layer

Figure 4 shows the block diagram of subalgorithm III, which is discussed below. It consists of:

**Section A** – the **Input data** essential for the computations include:

– $TOA(\lambda_i)$ (block 1) – satellite-measured upwelling radiance. It is often described as the water-leaving radiance at the top of the atmosphere. The data includes the influence of the atmosphere on the measured upwelling radiance. This effect is later removed during

the atmospheric corrections. At the current stage, the SeaWiFS and MODIS data are used in the process;

– ancillary data (block 2) that are later utilised, mainly in atmospheric corrections, e.g. meteorological data from NCEP and TOMS/TOAST ozone data.

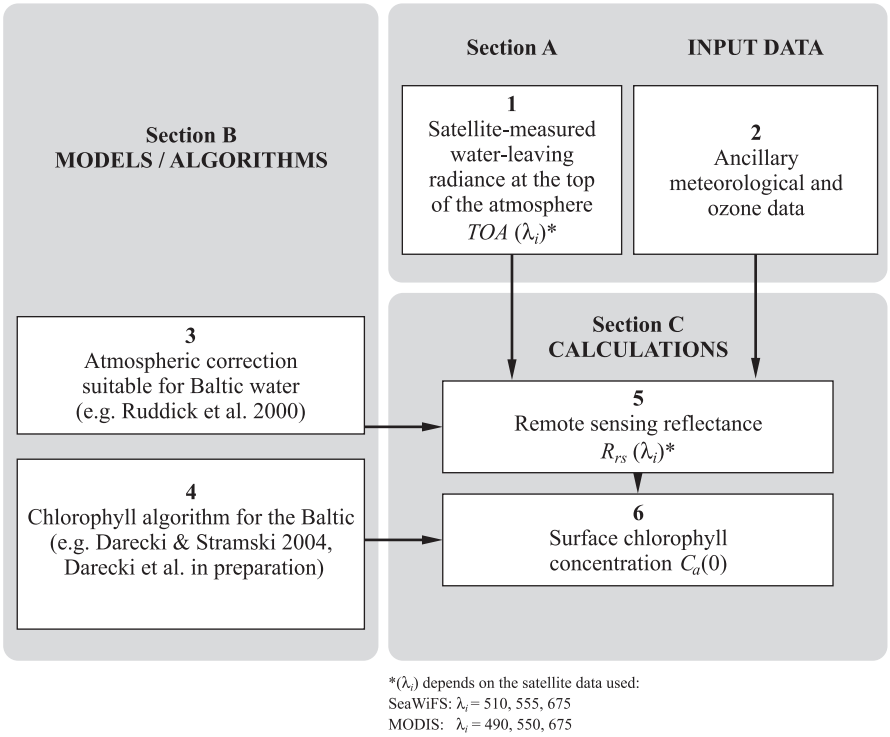


**Figure 4.** Block diagram of the subalgorithm for estimating the chlorophyll *a* concentration in the Baltic Sea surface layer (for the mathematical apparatus of this subalgorithm, see Annex III)

**Section B – Model formulae** contains a complex set of algorithms for

– atmospheric correction (block 3). Different algorithms can be applied here. In the present work, the authors used the atmospheric correction scheme proposed by Ruddick et al. (2000), which has proved to be the most suitable for the optically complex Baltic waters. It is very likely, however, that in the future new algorithms will be developed which will provide better results. In such a case the new algorithms should be applied here;

– estimating the chlorophyll *a* concentration in the surface layer based on the estimated water-leaving radiance or remotely sensed reflectance

(block 4). The chlorophyll algorithm, similar to the atmospheric correction, should take the Baltic's specific complexity into account (see Darecki & Stramski 2004, Darecki et al. 2005, in preparation).

**Section C – Calculations**. Using the input data (blocks 1–2) and the above procedures for the atmospheric correction in conjunction with the algorithms for estimating the chlorophyll *a* concentration (blocks 3–4) the following parameters are calculated in turn: the corrected remote sensing reflectance $R_{rs}(\lambda)$ in the relevant spectral channels (block 4), and then the chlorophyll *a* concentration in the surface layer of water (block 5).

A detailed description of the algorithm for the surface concentration of chlorophyll concentration in the Baltic will be found in Annex III.

## 2.4. Subalgorithm for calculating the daily dose of PAR transmitted across a wind-blown sea surface

Figure 5 shows a simplified block diagram for estimating the PAR dose transmitted across a wind-blown sea surface.

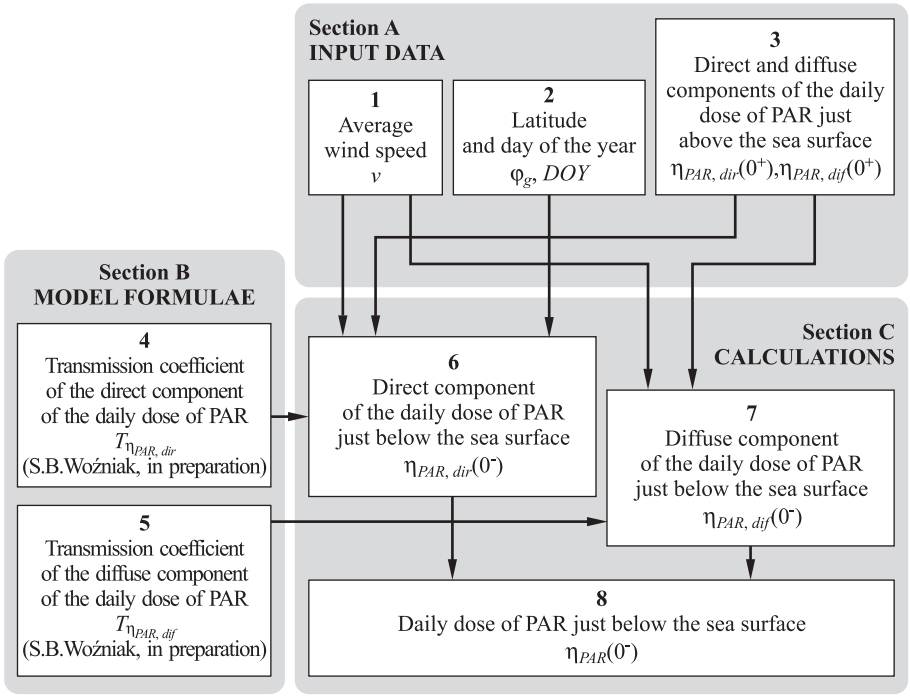


**Figure 5.** Block diagram of the subalgorithm for calculating the daily dose of PAR transmitted across a wind-blown sea surface (for the mathematical apparatus of this algorithm, see Annex IV)

Like the block diagrams for the three previous subalgorithms, this one, too, consists of three sections.

**Section A** – The **Input data** for calculating the dose of PAR transmitted across a wind-blown sea surface comprise the following magnitudes:

- $v$ (block 1) – the average wind speed above the water, which is the magnitude with respect to which the distribution of slopes on the wind-blown sea surface and the degree of foam coverage are parameterised;
- $\varphi_g$, $DOY$ (block 2) – latitude and the day number of the year, which characterise the time under scrutiny and the geographical location of the spot for which the PAR dose transmittance is calculated;
- $\eta_{PAR,\,dir}(0^+)$, $\eta_{PAR,\,dif}(0^+)$ (block 3) – the known distribution of the daily dose of PAR just above the sea surface, resolved into two components: a direct one (from direct solar radiation) and a diffuse one (from radiation scattered in the atmosphere).

**Section B** – The **Model Formulae** include: a simplified formula for the transmittance of the direct component of the PAR dose (block 4) and a simplified formula for the transmittance of the diffuse component of the same dose of PAR (block 5). In practice, these formulae make use of, among other things, the tabulated values of the reflection coefficients of the downward direct $R_d^{dir}$ and diffuse irradiance $R_d^{dif}$ (see Annex IV), as well as the set of simplifying assumptions concerning the possible courses of the daily variation in the surface irradiance by direct and diffuse light. The assumptions and mathematical procedures underpinning the results of modelling the transmittance of light across a wind-blown sea surface will be described in another paper currently being prepared for publication (see S. B. Woźniak, in preparation). At this point we merely indicate that the modelled values of the coefficients $R_d^{dir}$ and $R_d^{dif}$ used here take into account the interaction between the radiation incident from the sky and a wind-blown sea surface on the basis of the laws of geometrical optics, Snell's and Fresnel's Laws, and the roughness of the sea surface as characterised by the distribution of slopes of surface elements after Cox & Munk (1954). We only add that in calculating $R_d^{dif}$ the cardioidal formula for diffuse sky radiance distribution was taken into account (according to Mobley (1994); in the case of a heavily overcast sky the angular sky radiance distribution is approximately proportional to the following term: $(1 + 2\cos(\theta))$).

**Section C – Calculations**. The following magnitudes are calculated with the aid of the input data and model formulae: the values of the direct

component (block 6) and diffuse component (block 7) of the daily dose of PAR just below the sea surface, as well as the desired final value of the total dose of PAR just below the sea surface (block 8).

Annex IV details the precise mathematical apparatus of this subalgorithm.

### 2.5. Subalgorithm for estimating the underwater optical and bio-optical features and photosynthetic primary production in the Baltic Sea

This subalgorithm, the most complex of the components of the DESAMBEM algorithm for the Baltic, has a long history. The first version of this subalgorithm, published sixteen years ago, was based on the so-called 'light-photosynthesis' model (see Woźniak et al. 1992a,b) and was generally applicable to various sea and ocean waters. A few years later it was modified for application to the Baltic (see Dera 1995, Kaczmarek & Woźniak 1995, Woźniak & Olszewski 1995, Woźniak et al. 1995). Later still, the far more precise, second-generation 'light-photosynthesis' model, the MCM (Multicomponent Light-photosynthesis Model), was developed and empirically validated for oceanic case 1 waters (Ficek et al. 2003, Woźniak et al. 2003). Finally, the algorithm presented in this paper is based on a version of MCM that we modified for Baltic case 2 waters in 2003–07. It is presented graphically in Figure 6 and comprises the three sections discussed below.

**Section A** – the **Input data** essential for the computations include:

- $C_a(0)$ (block 1) – surface concentration of the total chlorophyll $a$;
- $PAR_0(0^-)$ (block 2) – irradiance (scalar) by sunlight in the PAR spectral range (400–700 nm) just below the sea surface;
- *temp* (block 3) – the sea surface temperature. For the sake of simplicity, we have assumed in this study a constant temperature throughout the photosynthetically active layer, just as in the mixed layer. This assumption may, of course, introduce some additional error to the primary production calculated for various depths in the sea. It can be demonstrated, however, that this error does not exceed 10%; it is negligible compared to the much larger error of the primary production empirical determination using the $C^{14}$ technique.

As has been mentioned, these three principal input data of the model (blocks 1–3) can be determined by satellite remote sensing. Additional information on the type of basin and the deep mixed layer should be considered in order to select some of the alternative equations of the model.

**Section B** contains a complex set of **Model formulae** taken from partial models. In detail, they are:

- (block 4) – a statistical model of the vertical distributions of chlorophyll in the Baltic $C_a(z)$, presented earlier by Ostrowska et al. (2007). The basic formula of this model links the chlorophyll $a$ concentrations at different depths with the surface concentration of this chlorophyll $C_a(0)$;
- (block 5) – the bio-optical underwater irradiance transmittance, which we developed earlier for oceanic case 1 waters (see Woźniak et al. 1992a,b) and then expanded to take account of Baltic case 2 waters (see Kaczmarek & Woźniak 1995). This model links various optical properties and the underwater light fields $E_d(\lambda, z)$ with the chlorophyll concentration at different depths $C_a(z)$ and the surface irradiance $PAR_0(0^-)$;
- (block 6) – the statistical model of photo- and chromatic acclimation containing model formulae defining the concentrations of individual photosynthetic and photoprotecting pigments in Baltic waters (Majchrowski et al. 2007). The formulae of this model link the concentrations of these various accessory pigments at different depths $C_j(z)$ with the concentration of chlorophyll $a$ $C_a(z)$ and the underwater irradiance fields;
- (block 7) – the model of light absorption by Baltic phytoplankton in vivo (Ficek et al. 2004), which takes account, among other things, of the pigment package effect in a cell and photo- and chromatic adaptation effects. The formulae of this model link various optical parameters characterising the light-absorption capacity of Baltic phytoplankton, and also the quantities of energy absorbed by phytoplankton and its several pigments, with the concentrations of these pigments $C_j(z)$ and the underwater irradiance fields;
- (block 8) – the model of the quantum efficiency of marine photosynthesis in the Baltic (Woźniak et al. 2007a,b), enabling this parameter to be determined from the above-mentioned input data, including surface chlorophyll $a$ as the trophic index of the waters in question, and the previously calculated magnitudes characterising the underwater light fields and the radiant energy absorbed by the photosynthetic and photoprotecting pigments in Baltic phytoplankton.

**Section C – Calculations** by applying the input data (blocks 1–3) and using the model formulae (blocks 4–8), calculations are now performed of a series of biotic and abiotic properties of the marine ecosystem, from the

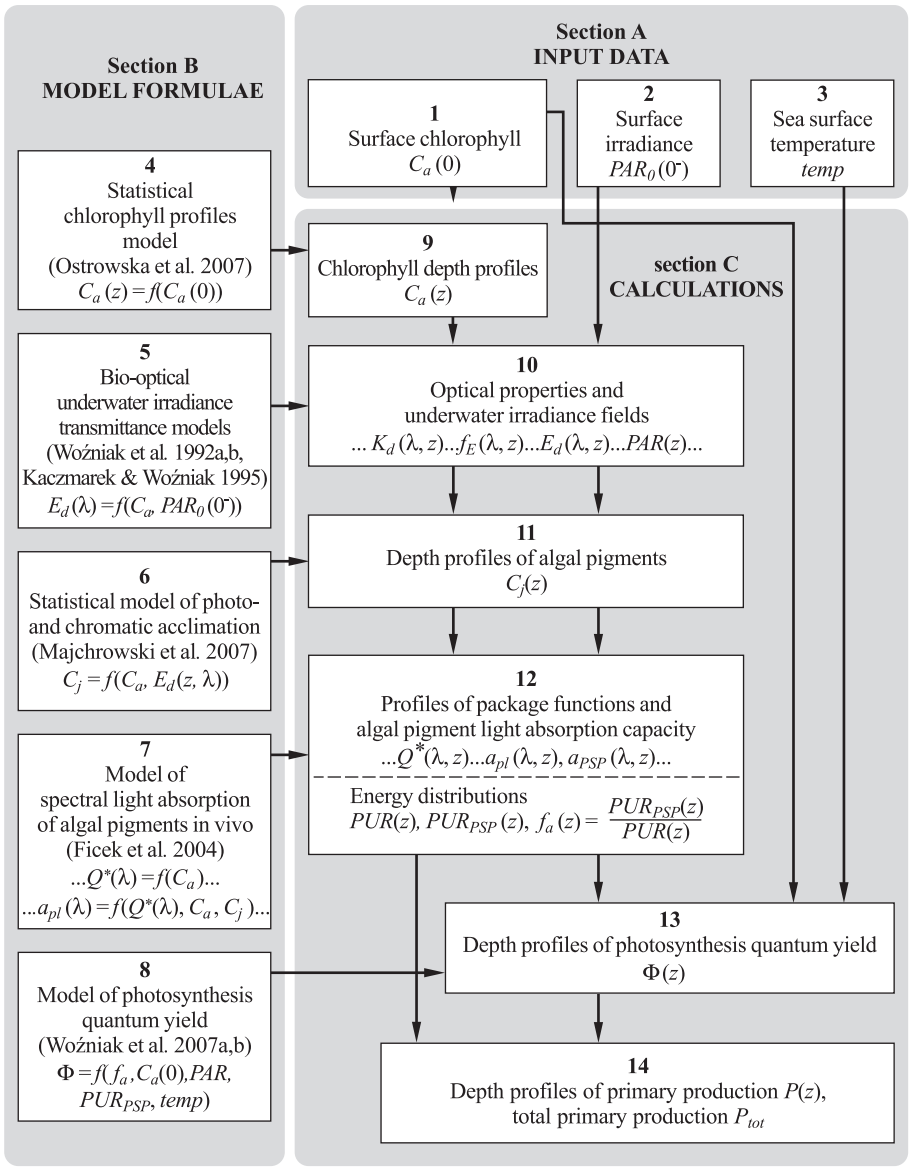


**Figure 6.** Block diagram of the subalgorithm for estimating the underwater optical and bio-optical features and photosynthetic primary production in the Baltic Sea (for the mathematical apparatus of this algorithm, see Annex V)

vertical distributions of the chlorophyll concentration $C_a(z)$ (block 9), to the vertical distributions of the quantum yield of photosynthesis $\Phi$(z) (block 13), and also of the primary production at various depths in the sea $P(z)$ and the total primary production in the water column $P_{tot}$ (block 14).

The entire algorithm of this general 'light-photosynthesis in the Baltic' model, set out in tabular form suitable for numerical programming, is given in Annex V. This algorithm merely presents the complete mathematical description of the problems analysed.

## 3. Summary

In the present paper we have shown that satellite data enable numerous properties of the Baltic Sea to be defined. Among them are the following, which can be estimated directly with the aid of the DESAMBEM algorithm: sea surface temperature, the Photosynthetically Available Radiation, the concentrations of chlorophyll and other pigments in the water, the photosynthetic efficiency and the primary production of organic matter. Moreover, as the monographs by Krężel (1997) and Robinson (1985) have shown, these directly determined features of the ecosystem allow other essential information on the marine environment to be obtained indirectly, for example, the distribution of upwelling currents, which can be determined from an analysis of maps of sea surface temperature. Once the algorithm has been expanded and made more precise, it will be possible to provide a whole range of other important information about the environment, such as an estimate of the intensity of UV radiation over the sea and in coastal regions, and distributions of the radiation balance between the sea surface and the upper layers of the atmosphere. These properties are therefore very important both for analysing the supply of energy to ecosystems and their functioning, as well as for climate modelling purposes.

Besides these advantages and the important role that the DESAMBEM algorithm may play in future studies of the Baltic Sea, we should, in all fairness, also mention two of its main drawbacks. Firstly, its applicability to the estimation of ecosystem parameters on the basis of remote sensing data – at least, in the version presented in this paper – is basically limited to such data obtained for a cloudless sky, i.e. when the optical observations by a satellite of particular pixels at sea are not partially or wholly hindered by the presence of clouds. Under such conditions the recorded satellite radiometer signals cannot be used directly for determining sea surface temperature or the surface concentration of chlorophyll. This is therefore quite a serious inconvenience as regards the practical applicability of this algorithm, because the average probability of clouds occurring over any random pixel in the Baltic, regardless of its position or the season of the year, is, according to our estimates, over 70%. Nonetheless, as we shall show in Part 2 (see Darecki et al. 2008 – this issue), it is possible to estimate these parameters (sea surface temperature and chlorophyll concentration) with a sufficiently high precision for areas of the sea where the sky is overcast if

one performs, using geostationary methods, the appropriate interpolations of their values between points in a time-space corresponding to cloudless states.

The second shortcoming of the DESAMBEM algorithm is the complexity of its mathematical structure, which in effect involves computations of relatively long duration when the full, unsimplified version of the algorithm is used. This comment applies especially to subalgorithm V (see Annex V and Figure 6), which enables the estimation of various ecosystem parameters on the basis of known values of the surface concentration of chlorophyll *a* $C_a(0)$, the sea surface temperature *temp* and the surface irradiance $PAR_0(0^-)$. To improve the operational efficiency of the DESAMBEM algorithm, and to produce maps of different parameters of the marine environment using it, we apply not the full 'light-photosynthesis in the sea' model, but its approximate and simplified polynomial version. We shall return to this problem in Part 2 (see Darecki et al. 2008 – this issue).

## References

Antoine D., André J. M., Morel A., 1996, *Oceanic primary production: 2. Estimation at global scale from satellite (coastal zone color scanner) chlorophyll*, Global Biogeochem. Cy., 10 (1), 56–69.

Antoine D., Morel A., 1996, *Oceanic primary production: 1. Adaptation of spectral light-photosynthesis model in view of application to satellite chlorophyll observations*, Global Biogeochem. Cy., 10 (1), 42–55.

Arst H., 2003, *Properties and remote sensing of multicomponental water bodies*, Springer–Praxis Publ. Ltd, Berlin–Chichester, 231 pp.

AVHRR Sea Surface Temperature Products, 2002, http://coastwatch.noaa.gov/poes_sst_algorithms.html

Bird R. E., Riordan C., 1986, *Simple solar spectral model for direct and diffuse irradiance on horizontal and tilted planes at the Earth's surface for cloudless atmospheres*, J. Clim. Appl. Meteorol., 25 (1), 87–97.

Campbell J., Antoine D., Armstrong R., Arrigo K., Balch W., Barber R., Behrenfeld M., Bidigare R., Bishop J., Carr M.-E., Esaias W., Falkowski P., Hoepffner N., Iverson R., Kieifer D., Lohrenz S., Marra J., Morel A., Ryan J., Vedernikov V., Waters K., Yentsch C., Yoder J., 2002, *Comparison of algorithms for estimating ocean primary production from surface chlorophyll, temperature, and irradience*, Global Biogeochem. Cy., 16 (3), 74–75.

Carr M.-E., Friedrichs M. A., Schmeltz M., Aita M. N., Antoine D., Arrigo K. R., Asanuma I., Aumont O., Barber R., Behrenfeld M., Bidigare R., Buitenhuis E. T., Campbell J., Ciotti A., Dierssen H., Dowell M., Dunne J., Esaias W., Gentili B., Gregg W., Groom S., Hoepffner N., Ishizaka J., Kameda T., Le Quéré C., Lohrenz S., Marra J., Mélin F., Moore K., Morel A., Reddy T. E., Ryan J., Scardi M., Smyth T., Turpie K., Tilstone G., Waters K.,

Yamanaka Y., 2006, *A comparison of global estimates of marine primary production from ocean color*, Deep Sea Res. Pt. II, 53, 741–770.

COSPAR International Reference Atmosphere (CIRA), 1996, Adv. Space Res., 18 (9/10), 11–58.

Cox C., Munk W. H., 1954, *Measurement of the sea surface from photographs of the Sun's glitter*, J. Opt. Soc. Am., 44 (11), 838–850.

Darecki M., Ficek D., Krężel A., Ostrowska M., Majchrowski R., Woźniak S. B., Bradtke K., Dera J., Woźniak B., 2008, *Algorithms for the remote sensing of the Baltic ecosystem (DESAMBEM). Part 2: Empirical validation*, Oceanologia, (this issue).

Darecki M., Kaczmarek S., Olszewski J., 2005, *SeaWiFS chlorophyll algorithms for the Southern Baltic*, Int. J. Remote Sens., 26 (2), 247–260.

Darecki M., Olszewski J., Kowalczuk P., Sagan S., *Regional optimization of retrieval of chlorophyll a concentration and CDOM absorption from remote sensing measurements in the Baltic Sea*, (in preparation).

Darecki M., Stramski D., 2004, *An evaluation of MODIS and SeaWiFS bio-optical algorithms in the Baltic Sea*, Remote Sens. Environ., 89 (3), 326–350.

Darecki M., Weeks A., Sagan S., Kowalczuk P., Kaczmarek S., 2003, *Optical characteristics of two contrasting Case 2 waters and their influence on remote sensing algorithms*, Cont. Shelf Res., 23 (3–4), 237–250.

Dera J., 1995, *Underwater irradiance as a factor affecting primary production*, Diss. and monogr. 7, Inst. Oceanol. PAS, Sopot, 110 pp.

Falkowski P. G., Knoll A. H. (eds.), 2007, *The evolution of aquatic photoautotrophs*, Acad. Press, New York, 456 pp.

Falkowski P. G., Raven J. A., 2007, *Aquatic photosynthesis*, 2nd edn., Princeton Univ. Press, Princeton, 484 pp.

Ficek D., Kaczmarek S., Stoń-Egiert J., Woźniak B., Majchrowski R., Dera J., 2004, *Spectra of light absorption by phytoplankton pigments in the Baltic; conclusions to be drawn from a Gaussian analysis of empirical data*, Oceanologia, 46 (4), 533–555.

Ficek D., Majchrowski R., Ostrowska M., Kaczmarek S., Woźniak B., Dera J., 2003, *Practical applications of the multi-component marine photosynthesis model (MCM)*, Oceanologia, 45 (3), 395–423.

Glantz M. H. (ed.) 1988, *Societal responses to regional climate change. Forecasting by analogy*, West View Press, Boulder–London, 403 pp.

Gordon H. R., Brown O. B., Evans R. H., Brown J. W., Smith R. C., Baker K. S., Clark D. K., 1988, *A semi-analytical radiance model of ocean color*, J. Geophys. Res., 93 (D9), 10909–10924.

Gordon H. R., Morel A., 1983, *Remote assesment of ocean color for interpretation of satellite visible imagery*, [in:] *Lecture notes on coastal and estuarine studies*, M. Bowman (ed.), Springer-Verlag, New York, 114 pp.

Gregg W. W., Carder K. L., 1990, *A simple spectral solar irradiance model for cloudless maritime atmosphere*, Limnol. Oceanogr., 35 (8), 1657–1675.

Hoots F. R., Roehrich R. L., 1988, *Models for propagations of NORAD elements set*, Spacetrack Rep. No. 3, http://www.amsat.org/amsat/ftp/docs/spacetrk.pdf

IOCCG, 2007, *Ocean-colour data merging*, W. W. Gregg (ed.), Rep. Int. Ocean-Colour Coordinating Group No. 6, IOCCG, Dartmouth (Canada).

Iqbal M., 1983, *An introduction to solar radiation*, Acad. Press, New York, 390 pp.

Jonasz M., Fournier G. R., 2007, *Light scattering by particles in water: Theoretical and experimental constraints*, Acad. Press, San Diego, CA, 714 pp.

Kaczmarek S., Woźniak B., 1995, *The application of the optical classification of waters in the Baltic Sea (Case 2 waters)*, Oceanologia, 37 (2), 285–297.

Kasten F., 1966, *A new table and approximate formula for relative optical mass*, Arch. Meteorol. Geophys. Bioclim., B14, 206–223.

Kneizys F. X., Shettle E. P., Gallery W. O., Chetwynd J. H., Jr., Abreu L. W., 1980, *Atmospheric transmittance/radiance: Computer code LOWTRAN5*, Tech. Rep. AFGL-TR-80-0067 USAF Geophys. Lab., Hanscom AFB, MA, 45 pp.

Koepke P., 1984, *Effective reflectance of oceanic whitecaps*, Appl. Opt., 23 (11), 1816–1824.

Kowalewski M., Krężel A., 2004, *System of automatic registration and geometric correction of AVHRR data*, Arch. Fotogram., Kartogr. Teledet., XIIIb, 397–407, (in Polish).

Krężel A., 1997, *Recognition of mesoscale hydrophysical anomalies in a shallow sea using broadband satellite remote sensing methods*, Diss. and monogr., Univ. Gd., Gdynia, 173 pp., (in Polish).

Krężel A., Kozłowski Ł., Paszkuta M., 2008, *A simple model of light transmission through the atmosphere over the Baltic Sea utilising satellite data*, Oceanologia, 50 (2), 125–146.

Krężel A., Kozłowski Ł., Szymanek L., Szymelfenig M., 2005, *Influence of coastal upwelling on chlorophyll-like pigments concentration in the surface water along the Polish coast of the Baltic Sea*, Oceanologia, 47 (4), 433–452.

Leckner B., 1978, *The spectral distribution of solar radiation at the earth's surface–elements of a model*, Sol. Energy, 20 (2), 143–150.

Lieth H., Whittaker R. H., 1975, *Primary productivity of the biosphere*, Springer -Verlag, Berlin–Heidelberg–New York, 339 pp.

Majchrowski R., Stoń-Egiert J., Ostrowska M., Woźniak B., Ficek D., Lednicka B., Dera J., 2007, *Remote sensing of vertical phytoplankton pigment distributions in the Baltic: new mathematical expressions. Part 2: Accessory pigment distribution*, Oceanologia, 49 (4), 491–511.

Mobley C. D., 1994, *Light and water: Radiative transfer in natural waters*, Acad. Press, San Diego, CA, 592 pp.

Monahan E. C., O'Muircheartaigh I. G., 1986, *Whitecaps and the passive remote sensing of the ocean surface*, Int. J. Remote Sens., 7 (5), 627–642.

Morel A., Prieur L., 1977, *Analysis of variations in ocean color*, Limnol. Oceanogr., 22 (4), 709–722.

Neckel H., Labs D., 1981, *Improved data of solar spectral irradiance from 0.33 to 1.25 $\mu m$*, Sol. Phys., 74 (1), 231–249.

NOAA KLM, 2005, *User's guide. Appendix G.3*, http://www2.ncdc.noaa.gov/docs/klm/html/g/app-g3.htm

Ostrowska M., Majchrowski R., Stoń-Egiert J., Woźniak B., Ficek D., Dera J., 2007, *Remote sensing of vertical phytoplankton pigment distributions in the Baltic: new mathematical expressions. Part 1: Total chlorophyll a distribution*, Oceanologia, 49 (4), 471–489.

Platt T., Sathyendranath S., 1993a, *Estimators of primary production for interpretation of remotely sensed data on ocean color*, J. Geophys. Res.-Oceans, 98 (C8), 14561–14576.

Platt T., Sathyendranath S., 1993b, *The remote sensing of ocean primary productivity – use of a new data compilation to test satellite algorithms – comment*, J. Geophys. Res.-Oceans, 98, 16583–16584.

Platt T., Sathyendranath S., Cavarhill C. M., Lewis M. R., 1988, *Ocean primary production and available light: further algorithms for remote sensing*, Deep-Sea Res. Pt. I, 35 (6), 855–879.

Platt T., Sathyendranath S., Longhurst A., 1995, *Remote-sensing of primary production in the ocean – promise and fulfilment*, Phil. T. Roy. Soc. B, 348, 191–201.

Reitan G. H., 1960, *Mean monthly values of precipitable water over the United States*, Mon. Weather Rev., 88, 25–35.

Robinson I. S., 1985, *Satellite oceanography*, Ellis Horwood, Chichester, 455 pp.

Ruddick K. G., Ovidio F., Rijkeboer M., 2000, *Atmospheric correction of SeaWiFS imagery for turbid coastal and inland waters*, Appl. Opt., 39 (6), 897–912.

Sathyendranath S., Cota G., Stuart V., Maass H., Platt T., 2001, *Remote sensing of phytoplankton pigments: a comparison of empirical and theoretical approaches*, Int. J. Remote Sens., 22 (2–3), 249–273.

Sathyendranath S., Hoge F. E., Platt T., Swift R. N., 1994, *Detection of phytoplankton pigments from ocean color – improved algorithms*, Appl. Opt., 33 (6), 1081–1089.

Sathyendranath S., Platt T., Cavarhill C. M., Warnock R. E., Lewis M. R., 1989, *Remote sensing of oceanic primary production: computations using a spectral model*, Deep-Sea Res., 36 (3), 431–453.

Sathyendranath S., Platt T., Stuart V., 2000, *Remote sensing of ocean colour: Recent advances, exciting possibilities and unanswered questions*, Proc. 5th Pacific Ocean Remote Sens. Conf. (PORSEC), Dona Paula, Goa, 5–8 Dec. 2000, Vol. 1, p. 6.

Spencer J. W., 1971, *Fourier series representation of the position of the Sun*, Search, 2 (5), 172.

Steemann Nielsen E., 1975, *Marine photosynthesis with special emphasis on the ecological aspect*, Elsevier, Amsterdam, 141 pp.

Trenberth K. E. (ed.), 1992, *Climate system modelling*, Cambridge Univ. Press, Cambridge, 788 pp.

Woźniak B., Dera J., 2007, *Light absorption in sea water*, Atmos. Oceanogr. Sci. Libr. 33, Springer, New York, 454 pp.

Woźniak B., Dera J., Ficek D., Majchrowski R., Ostrowska M., Kaczmarek S., 2003, *Modelling light and photosynthesis in the marine environment*, Oceanologia, 45 (2), 171–245.

Woźniak B., Dera J., Koblentz-Mishke O. I., 1992a, *Bio-optical relationships for estimating primary production in the Ocean*, Oceanologia, 33, 5–38.

Woźniak B., Dera J., Koblentz-Mishke O. I., 1992b, *Modelling the relationship between primary production, optical properties, and nutrients in the sea*, Ocean Optics 11, Proc. SPIE, 1750, 246–275.

Woźniak B., Dera J., Semovski S., Hapter R., Ostrowska M., Kaczmarek S., 1995, *Algorithm for estimating primary production in the Baltic by remote sensing*, Stud. Mater. Oceanol., 68 (Mar. Phys. 8), 91–123.

Woźniak B., Ficek D., Ostrowska M., Majchrowski R., Dera J., 2007a, *Quantum yield of photosynthesis in the Baltic: a new mathematical expression for remote sensing applications*, Oceanologia, 49 (4), 527–542.

Woźniak B., Hapter R., 1985, *Statisticheskii analiz rezultatov mnogoletnikh nabliudenii nad postupleniem solnechnoi energii v evfoticheskuiu zonu iuzhnoi Baltiki*, [in:] *Utilisation of solar energy in the photosynthesis of the Baltic and Black Sea phytoplankton*, O. I. Koblentz-Mishke, B. Woźniak & Yu. E. Ochakovskiy (eds.), Izd. IO AN SSSR, Moskva, 176–204, (in Russian).

Woźniak B., Krężel A., Dera J., 2004, *Development of a satellite method for Baltic ecosystem monitoring* (*DESAMBEM*) – *an ongoing project in Poland*, Oceanologia, 46 (3), 445–455.

Woźniak B., Majchrowski R., Ostrowska M., Ficek D., Kunicka J., Dera J., 2007b, *Remote sensing of vertical phytoplankton pigment distributions in the Baltic: new mathematical expressions. Part 3: Non-photosynthetic pigment absorption factor*, Oceanologia, 49 (4), 513–526.

Woźniak B., Olszewski J., 1995, *Introduction to remote methods of evaluation of primary production in the Baltic*, Stud. Mater. Oceanol., 68 (Mar. Phys. 8), 3–13.

Woźniak S. B., *Simple method for estimation the transmission of the daily dose of PAR across a wind-blown sea surface*, (in preparation).

## Annex I. Mathematical apparatus of the subalgorithm for estimating the irradiance at the Baltic Sea surface

### Section A

The **input parameters** of the model are: day of the year – $DOY$, Greenwich Mean Time – $GMT$, longitude E – $\lambda_g$, latitude N – $\varphi_g$ (**Block 1**); meteorological data at sea level: water vapour pressure – $e$ [hP], atmospheric pressure – $p$ [hP], air temperature just above the sea surface – $T$ [°C] (**Block 2**); upward radiance at the satellite level in spectral channels $\lambda$ – $L_u$, satellite-derived aerosol optical thickness – $\tau_a$ (**Block 3**).

### Section B

**The model formulae are:**

**Block 4 – Sun-Earth geometry formulae (according to Spencer 1971, Krężel 1997)**:

- Solar zenith angle:

$$\theta_{\otimes} = \arccos[\sin\varphi_G \sin\delta_{\otimes} + \cos\varphi_G \cos\delta_{\otimes} \cos(15t_{\otimes} - 180)], \quad \text{(AI.1)}$$

where $t_{\otimes}$ – real solar time:

$$t_{\otimes} = \pi\left(\frac{GMT}{12} - 1 - \frac{\lambda_g}{180}\right) + EoT, \quad \text{(AI.2)}$$

$\delta_{\otimes}$ – declination of the Sun (Spencer 1971):

$$\delta_{\otimes} = 0.006918 - 0.399912\cos\psi + 0.070257\sin\psi - \\ -0.006758\cos 2\psi + 0.000907\sin 2\psi - 0.002697\cos 3\psi + \\ +0.001480\sin 3\psi, \quad \text{(AI.3)}$$

$EoT$ – equation of time (Spencer 1971):

$$EoT = 0.00075 + 0.001868\cos\psi - 0.032077\sin\psi - \\ -0.014615\cos 2\psi - 0.040849\sin 2\psi, \quad \text{(AI.4)}$$

$$\psi = \frac{2\pi(DOY - 1)}{365}, \quad \text{(AI.5)}$$

where $DOY = 1$ for 1 January, 2 for 2 January ..., 365 for 31 December.

- Ratio of the mean ($\overline{R}$) to actual ($R$) Sun-Earth distance, $\beta = \frac{\overline{R}^2}{R^2}$. The reciprocal of this value is (Spencer 1971):

$$\beta^{-1} = 1.00011 + 0.034221\cos\psi + 0.00128\sin\psi + \\ +0.000719\cos 2\psi + 0.000077\sin 2\psi. \quad \text{(AI.6)}$$

**Block 5 – relationships for estimating the following optical quantities (according to Reitan 1960, Kasten 1966, Leckner 1978, Kneizys et al. 1980, Bird & Riodan 1986, Krężel 1997):**

- The transmission factor of solar radiation associated with the latter's Rayleigh scattering by atmospheric gases (Kneizys et al. 1980):

$$T_R(\lambda) = \exp\left\{-M\frac{p}{p_0}[\lambda^{-4}(115.6406 - 1.335\lambda^{-2})]\right\}, \tag{AI.7}$$

where $p_0 = 1013$ hP, $p$ is expressed in [hP] and $\lambda$ in [$\mu$m], and M is the total optical mass of the atmosphere (Kasten 1966):

$$M = [\cos\theta_\otimes + 0.15(93.835 - \theta_\otimes)^{-1.253}]^{-1}\sqrt{a^2 + b^2}. \tag{AI.8}$$

- The transmission factor of solar radiation associated with the latter's absorption by the water vapour content in the atmosphere (Leckner 1978):

$$T_W(\lambda) = \exp\left\{\frac{-0.2385a_w(\lambda)WM}{[1 + 20.07a_w(\lambda)WM]^{0.45}}\right\}, \tag{AI.9}$$

where the water vapour mass in an atmospheric air column of unit base area $W$ is calculated from the data on water vapour pressure $e_0$ at sea level, according to the relation (Reitan 1960):

$$W = (0.123 + 0.152e_0)\frac{p}{1000}, \tag{AI.10}$$

$e_0$ and the atmospheric pressure $p$ in (B10) are expressed in [hP]. Table AI.2 gives values of $a_w$, $a_{O_3}$, and $a_u$.

- The transmission factor of solar radiation associated with the latter's absorption by ozone:

$$T_{O_3}(\lambda) = \exp[-a_{O_3}(\lambda)O_3M_{O_3}], \tag{AI.11}$$

where the relative optical mass of atmospheric ozone $M_{O_3}$ is defined after Iqbal (1983) as

$$M_{O_3} = \frac{\left(1 + \dfrac{h_{O_3}}{6370}\right)}{\left(\cos^2\theta_\otimes + \dfrac{2h_{O_3}}{6370}\right)^{0.5}} \tag{AI.12}$$

and $h_{O_3}$, the height of maximum ozone concentration, is taken to be 22 km. Table AI.1 gives average ozone concentrations in the Baltic atmosphere.

- Components $T_{aa}$ and $T_{as}$ of the transmision function of solar radiation associated with the latter's attenuation by the aerosol:

$$T_{as}(\lambda) = \exp[-\omega_0(\lambda)\tau_a(\lambda)M], \tag{AI.13}$$

$$T_{aa}(\lambda) = \exp\{-[1-\omega_0(\lambda)]\tau_a(\lambda)M\}, \tag{AI.14}$$

where the spectral aerosol optical thickness ($\tau_a(\lambda)$) and single scattering albedo for the aerosol ($\omega_0(\lambda)$) are:

$$\tau_a(\lambda) = 0.742\tau_a(630)a\exp[b(\lambda)], \tag{AI.15}$$

where $a = 1.63$,

$\tau_a(630)$ – aerosol optical thickness taken from
http://www.class.noaa.gov/saa/products/search?sub_id=0&_data-type_family=AERO100&submit.x=18&submit.y=10,

$$b(\lambda) = 4.588\ \exp(-2.981\lambda/1000). \tag{AI.16}$$

$$\omega_0(\lambda) = \omega_0(0.4\,\mu\mathrm{m})\exp\left[-\omega'\left(\ln\frac{\lambda}{0.4}\right)^2\right], \tag{AI.17}$$

$\omega_0(0.4) = 0.945$ and $\omega' = 0.095$.

- The transmission factor of solar radiation associated with the latter's absorption by the other significant components of the atmosphere (Leckner 1978):

$$T_G(\lambda) = \exp\left[\frac{-1.41a_u(\lambda)M\,p\,p_0^{-1}}{\left[1+118.3a_u(\lambda)M\,p\,p_0^{-1}\right]^{0.45}}\right]. \tag{AI.18}$$

- The total transmission factor of direct solar irradiance in a cloudless atmosphere:

$$T^0 = T^R(\lambda)T_W(\lambda)T_{O_3}(\lambda)T_G(\lambda)T_{aa}(\lambda). \tag{AI.19}$$

- The scattered radiation reaching the sea surface (Bird & Riordan 1986):

$$E_{\downarrow dif}(\lambda) = [E_{dR}(\lambda) + E_{da}(\lambda) + E_{dg}(\lambda)]C, \tag{AI.20}$$

where the components of this sum are defined as:

$$E_{dR}(\lambda) = F_{\otimes}(\lambda)\beta^{-1}\cos\theta T_{O_3}(\lambda)T_G(\lambda)T_w(\lambda)T_{aa}(\lambda)\times$$
$$\times[1-T_R(\lambda)^{0.95}]0.5, \tag{AI.21}$$

$$E_{da}(\lambda) = F_{\otimes}(\lambda)\beta^{-1}\cos\theta T_{O_3}(\lambda)T_G(\lambda)T_w(\lambda)T_{aa}(\lambda)\times$$
$$\times T_R(\lambda)^{1.5}[1 - T_{as}(\lambda)]F, \tag{AI.22}$$

$$E_{dg}(\lambda) = \frac{[F_{\otimes}(\lambda)\cos\theta + E_{dR} + E_{da}(\lambda)]r_s(\lambda)r_g(\lambda)}{1 - r_s(\lambda)r_g(\lambda)}, \tag{AI.23}$$

where $F_{\otimes}$ – spectral density of the solar constant given in Table AI.2,

$$r_s(\lambda) = T'_{O_3}(\lambda)T'_w(\lambda)T'_{aa}(\lambda)\{0.5[1 - T'_R(\lambda)] + (1 - F')T'_R(\lambda)\times$$
$$\times[1 - T'_{as}(\lambda)]\}, \tag{AI.24}$$

$$F = 1 - 0.5\exp[(AFS + BFS\cos\theta_{\otimes})\cos\theta_{\otimes}], \tag{AI.25}$$

$$AFS = ALG[1.459 + ALG(0.1595 + ALG \times 0.4129)], \tag{AI.26}$$

$$ALG = \ln(1 - <\cos\theta_{\otimes}>), \tag{AI.27}$$

$$BFS = ALG[0.0783 + ALG(-0.3824 - ALG \times 0.5874)], \tag{AI.28}$$

$$<\cos\theta_{\otimes}> = 0.65.$$

The primed parameters in equation (AI.23) were calculated by applying $M = 1.8$, and in the formula by defining $F - \cos\theta_{\otimes} = \dfrac{1}{1.8}$,

$$C = \begin{cases} (\lambda + 0.55)^{0.8} & \text{for } \lambda \le 0.45\ \mu\text{m} \\ 1.0 & \text{for } \lambda > 0.45\ \mu\text{m}. \end{cases} \tag{AI.29}$$

The albedo of the sea area $r_g$ was assumed constant and equal to 0.06.

**Block 6 – relationship for estimating the transmittance of solar radiation in a real terrestrial atmosphere (completely or partly covered by clouds) (Krężel et al. 2008):**

$$T^r(c_T) = 1 - ac_T - bc_T^2, \tag{AI.30}$$

where the cloudiness coefficient $c_T$, is defined as

$$c_T = \begin{cases} 0 & \text{for } A_s \le 0.091 \\ \dfrac{A_s - 0.091}{(0.53 + 0.0027\,\theta_{\otimes}) - 0.091} & \text{for } 0.091 < A_s \le 0.53 + 0.0027\,\theta_{\otimes} \\ 1 & \text{for } A_s > 0.53 + 0.0027\,\theta_{\otimes}, \end{cases} \tag{AI.31}$$

where
$A_S(\lambda) = \dfrac{L_u(\lambda)}{F_{\otimes}(\lambda)}$ – satellite-derived (Meteosat – SEVIRI) terrestrial albedo, $\theta_{\otimes}$ – solar zenith angle and $L_u(\lambda)$ – upward radiance at satellite level.

**Section C**

**The principles of the computations are:**

**Block 7 – The spectral solar downward irradiance outside the atmosphere is determined from the relationship**

$$E_{\downarrow 0}(\lambda) = \frac{F_{\otimes}(\lambda)}{\beta} \cos\theta_{\otimes}, \tag{AI.32}$$

where $\beta$ and $\theta_{\otimes}$ can be calculated from input data ($DOY$, GMT, $\lambda_g$ and $\varphi_g$) using equations (AI.1)–(AI.6).

**Block 8 – The spectral solar downward irradiances $E_{\downarrow dir}$ (direct), $E_{\downarrow dif}$ (scattered) and $E_{\downarrow \otimes S}$ (sum) at sea level under cloudless conditions are determined from the relationships**

$$E_{\downarrow dir}(\lambda) = E_{\downarrow 0}(\lambda) T^0(\lambda), \tag{AI.33}$$

$E_{\downarrow dif}$ – see equation (AI.20),

$$E_{\downarrow \otimes S}(\lambda) = E_{\downarrow 0}(\lambda) T^0(\lambda) + E_{\downarrow dif}(\lambda) \tag{AI.34}$$

on the basis of the magnitude $E_{d\downarrow 0}$ determined earlier and taking the various optical parameters of the atmosphere described by equations (AI.7)–(AI.29) into consideration.

**Block 9 – The spectral solar downward irradiances $E_{\downarrow dir,\, real}$ (direct), $E_{\downarrow dif,\, real}$ (scattered) and $E_{\downarrow S}$ (sum) at the sea surface under real atmospheric conditions are determined from the relationships**

$$E_{\downarrow dir,\, real}(\lambda) = E_{\downarrow dir}(\lambda) T^r, \tag{AI.35}$$

$$E_{\downarrow dif,\, real}(\lambda) = E_{\downarrow dif}(\lambda) T^r, \tag{AI.36}$$

$$E_{\downarrow S}(\lambda) = E_{\downarrow \otimes S}(\lambda) T^r, \tag{AI.37}$$

i.e. on the basis of the values of $E_{\downarrow dir}$, $E_{\downarrow dif}$ and $E_{\downarrow \otimes S}$ determined earlier and taking into account the transmittance of the solar radiation in a real terrestrial atmosphere $T^r$, described by equations (AI.30) and (AI.31).

The downward irradiances $E_{\downarrow dir,real}$, $E_{\downarrow dif,real}$ and $E_{\downarrow S}$ determined as above denote the instantaneous values of the spectral densities of the solar radiation energy incident on the sea surface (direct, diffuse and total, respectively), expressed in units of power. On the other hand, the corresponding values of these energies with respect to the total, not spectral, irradiances (e.g. in the PAR spectral interval, i.e. 400–700 nm), or the values of their doses in finite intervals of time (e.g. the daily irradiation), can be obtained by appropriately integrating these instantaneous spectral energy densities over the radiation wavelength and/or over time.

**Table AI.1.** Mean ozone concentration, $O_3$ in the atmosphere in the Baltic Sea area (COSPAR 1996)

| Month | Jan. | Feb. | Mar. | Apr. | May | June | July | Aug. | Sept. | Oct. | Nov. | Dec. |
|---|---|---|---|---|---|---|---|---|---|---|---|---|
| $O_3$ [cm] | 0.38 | 0.42 | 0.42 | 0.41 | 0.39 | 0.37 | 0.34 | 0.32 | 0.31 | 0.31 | 0.32 | 0.35 |

**Table AI.2.** Spectral density of the solar constant and absorption coefficients of water vapour – $a_w$, ozone – $a_{O_3}$ and other important gaseous components – $a_u$ of the atmosphere (Neckel & Labs 1981)

| $(\lambda)$ [nm] | $F_{\otimes}(\lambda)$ [W m$^{-2}\mu$m$^{-1}$] | $a_w(\lambda)$ [m$^{-1}$] | $a_{O_3}(\lambda)$ [m$^{-1}$] | $a_u(\lambda)$ [m$^{-1}$] | $(\lambda)$ [nm] | $F_{\otimes}(\lambda)$ [W m$^{-2}\mu$m$^{-1}$] | $a_w(\lambda)$ [m$^{-1}$] | $a_{O_3}(\lambda)$ [m$^{-1}$] | $a_u(\lambda)$ [m$^{-1}$] |
|---|---|---|---|---|---|---|---|---|---|
| 300.0 | 535.9 | 0.0 | 10.0 | 0.0 | 980.0 | 767.0 | 1.48 | 0.0 | 0.0 |
| 305.0 | 558.3 | 0.0 | 4.80 | 0.0 | 993.5 | 757.6 | 0.1 | 0.0 | 0.0 |
| 310.0 | 622.0 | 0.0 | 2.70 | 0.0 | 1040.0 | 688.1 | 0.00001 | 0.0 | 0.0 |
| 315.0 | 692.7 | 0.0 | 1.35 | 0.0 | 1070.0 | 640.7 | 0.001 | 0.0 | 0.0 |
| 320.0 | 715.1 | 0.0 | 0.800 | 0.0 | 1100.0 | 606.2 | 3.2 | 0.0 | 0.0 |
| 325.0 | 832.9 | 0.0 | 0.380 | 0.0 | 1120.0 | 585.9 | 115.0 | 0.0 | 0.0 |
| 330.0 | 961.9 | 0.0 | 0.116 | 0.0 | 1130.0 | 570.2 | 70.0 | 0.0 | 0.0 |
| 335.0 | 931.9 | 0.0 | 0.075 | 0.0 | 1145.0 | 564.1 | 75.0 | 0.0 | 0.0 |
| 340.0 | 900.6 | 0.0 | 0.040 | 0.0 | 1161.0 | 544.2 | 10.0 | 0.0 | 0.0 |
| 345.0 | 911.3 | 0.0 | 0.019 | 0.0 | 1170.0 | 533.4 | 5.0 | 0.0 | 0.0 |
| 350.0 | 975.5 | 0.0 | 0.007 | 0.0 | 1200.0 | 501.6 | 2.0 | 0.0 | 0.0 |
| 360.0 | 975.9 | 0.0 | 0.0 | 0.0 | 1240.0 | 477.5 | 0.002 | 0.0 | 0.05 |
| 370.0 | 1119.9 | 0.0 | 0.0 | 0.0 | 1270.0 | 442.7 | 0.002 | 0.0 | 0.30 |
| 380.0 | 1103.8 | 0.0 | 0.0 | 0.0 | 1290.0 | 440.0 | 0.1 | 0.0 | 0.02 |
| 390.0 | 1033.8 | 0.0 | 0.0 | 0.0 | 1320.0 | 416.8 | 4.0 | 0.0 | 0.0002 |
| 400.0 | 1479.1 | 0.0 | 0.0 | 0.0 | 1350.0 | 391.4 | 200.0 | 0.0 | 0.00011 |
| 410.0 | 1701.3 | 0.0 | 0.0 | 0.0 | 1395.0 | 358.9 | 1000.0 | 0.0 | 0.00001 |
| 420.0 | 1740.4 | 0.0 | 0.0 | 0.0 | 1442.5 | 327.5 | 185.0 | 0.0 | 0.05 |
| 430.0 | 1587.2 | 0.0 | 0.0 | 0.0 | 1462.5 | 317.5 | 80.0 | 0.0 | 0.011 |

**Table AI.2.** (*continued*)

| $(\lambda)$ [nm] | $F_{\otimes}(\lambda)$ [W m$^{-2}\mu$m$^{-1}$] | $a_w(\lambda)$ [m$^{-1}$] | $a_{O_3}(\lambda)$ [m$^{-1}$] | $a_u(\lambda)$ [m$^{-1}$] | $(\lambda)$ [nm] | $F_{\otimes}(\lambda)$ [W m$^{-2}\mu$m$^{-1}$] | $a_w(\lambda)$ [m$^{-1}$] | $a_{O_3}(\lambda)$ [m$^{-1}$] | $a_u(\lambda)$ [m$^{-1}$] |
|---|---|---|---|---|---|---|---|---|---|
| 440.0 | 1837.0 | 0.0 | 0.0 | 0.0 | 1477.0 | 307.3 | 80.0 | 0.0 | 0.005 |
| 450.0 | 2005.0 | 0.0 | 0.003 | 0.0 | 1497.0 | 300.4 | 12.0 | 0.0 | 0.0006 |
| 460.0 | 2043.0 | 0.0 | 0.006 | 0.0 | 1520.0 | 292.8 | 0.16 | 0.0 | 0.0 |
| 470.0 | 1987.0 | 0.0 | 0.009 | 0.0 | 1539.0 | 275.5 | 0.002 | 0.0 | 0.005 |
| 480.0 | 2027.0 | 0.0 | 0.014 | 0.0 | 1558.0 | 272.1 | 0.0005 | 0.0 | 0.13 |
| 490.0 | 1896.0 | 0.0 | 0.021 | 0.0 | 1578.0 | 259.3 | 0.0001 | 0.0 | 0.04 |
| 500.0 | 1909.0 | 0.0 | 0.030 | 0.0 | 1592.0 | 246.9 | 0.00001 | 0.0 | 0.06 |
| 510.0 | 1927.0 | 0.0 | 0.040 | 0.0 | 1610.0 | 244.0 | 0.0001 | 0.0 | 0.13 |
| 520.0 | 1831.0 | 0.0 | 0.048 | 0.0 | 1630.0 | 243.5 | 0.001 | 0.0 | 0.001 |
| 530.0 | 1891.0 | 0.0 | 0.063 | 0.0 | 1646.0 | 234.8 | 0.01 | 0.0 | 0.0014 |
| 540.0 | 1898.0 | 0.0 | 0.075 | 0.0 | 1678.0 | 220.5 | 0.036 | 0.0 | 0.0001 |
| 550.0 | 1892.0 | 0.0 | 0.085 | 0.0 | 1740.0 | 190.8 | 1.1 | 0.0 | 0.00001 |
| 570.0 | 1840.0 | 0.0 | 0.120 | 0.0 | 1800.0 | 171.1 | 130.0 | 0.0 | 0.00001 |
| 593.0 | 1768.0 | 0.075 | 0.119 | 0.0 | 1860.0 | 144.5 | 1000.0 | 0.0 | 0.0001 |
| 610.0 | 1728.0 | 0.0 | 0.120 | 0.0 | 1920.0 | 135.7 | 500.0 | 0.0 | 0.001 |
| 630.0 | 1658.0 | 0.0 | 0.090 | 0.0 | 1960.0 | 123.0 | 100.0 | 0.0 | 4.3 |
| 656.0 | 1524.0 | 0.0 | 0.065 | 0.0 | 1985.0 | 123.8 | 4.0 | 0.0 | 0.20 |
| 667.6 | 1531.0 | 0.0 | 0.051 | 0.0 | 2005.0 | 113.0 | 2.9 | 0.0 | 21.0 |
| 690.0 | 1420.0 | 0.016 | 0.028 | 0.15 | 2035.0 | 108.5 | 1.0 | 0.0 | 0.13 |
| 710.0 | 1399.0 | 0.0125 | 0.018 | 0.0 | 2065.0 | 97.5 | 0.4 | 0.0 | 1.0 |
| 718.0 | 1374.0 | 1.80 | 0.015 | 0.0 | 2100.0 | 92.4 | 0.22 | 0.0 | 0.08 |
| 724.4 | 1373.0 | 2.5 | 0.012 | 0.0 | 2148.0 | 82.4 | 0.25 | 0.0 | 0.001 |
| 740.0 | 1298.0 | 0.061 | 0.010 | 0.0 | 2198.0 | 74.6 | 0.33 | 0.0 | 0.00038 |
| 752.5 | 1269.0 | 0.0008 | 0.008 | 0.0 | 2270.0 | 68.3 | 0.50 | 0.0 | 0.001 |
| 757.5 | 1245.0 | 0.0001 | 0.007 | 0.0 | 2360.0 | 63.8 | 4.0 | 0.0 | 0.0005 |
| 762.5 | 1223.0 | 0.00001 | 0.006 | 4.0 | 2450.0 | 49.5 | 80.0 | 0.0 | 0.00015 |
| 767.5 | 1205.0 | 0.00001 | 0.005 | 0.35 | 2500.0 | 48.5 | 310.0 | 0.0 | 0.00014 |
| 780.0 | 1183.0 | 0.0006 | 0.0 | 0.0 | 2600.0 | 38.6 | 15000.0 | 0.0 | 0.00066 |
| 800.0 | 1148.0 | 0.0360 | 0.0 | 0.0 | 2700.0 | 36.6 | 22000.0 | 0.0 | 100.0 |
| 816.0 | 1091.0 | 1.60 | 0.0 | 0.0 | 2800.0 | 32.0 | 8000.0 | 0.0 | 150.0 |
| 823.7 | 1062.0 | 2.5 | 0.0 | 0.0 | 2900.0 | 28.1 | 650.0 | 0.0 | 0.13 |
| 831.5 | 1038.0 | 0.500 | 0.0 | 0.0 | 3000.0 | 24.8 | 240.0 | 0.0 | 0.0095 |
| 840.0 | 1022.0 | 0.155 | 0.0 | 0.0 | 3100.0 | 22.1 | 230.0 | 0.0 | 0.001 |
| 860.0 | 998.7 | 0.00001 | 0.0 | 0.0 | 3200.0 | 19.6 | 100.0 | 0.0 | 0.8 |
| 880.0 | 947.2 | 0.0026 | 0.0 | 0.0 | 3300.0 | 17.5 | 120.0 | 0.0 | 1.9 |
| 905.0 | 893.2 | 7.0 | 0.0 | 0.0 | 3400.0 | 15.7 | 19.5 | 0.0 | 1.3 |
| 915.0 | 868.2 | 5.0 | 0.0 | 0.0 | 3500.0 | 14.1 | 3.6 | 0.0 | 0.075 |
| 925.0 | 829.7 | 5.0 | 0.0 | 0.0 | 3600.0 | 12.7 | 3.1 | 0.0 | 0.01 |
| 930.0 | 830.3 | 27.0 | 0.0 | 0.0 | 3700.0 | 11.5 | 2.5 | 0.0 | 0.00195 |
| 937.0 | 814.0 | 55.0 | 0.0 | 0.0 | 3800.0 | 10.4 | 1.4 | 0.0 | 0.004 |
| 948.0 | 786.9 | 45.0 | 0.0 | 0.0 | 3900.0 | 9.5 | 0.17 | 0.0 | 0.29 |
| 965.0 | 768.3 | 4.0 | 0.0 | 0.0 | 4000.0 | 8.6 | 0.0045 | 0.0 | 0.025 |

## Annex II. Mathematical apparatus of the subalgorithm for estimating the Baltic Sea surface temperature

### Section A

The **input parameters** of the model are: Greenwich Mean Time – $GMT$, longitude E – $\lambda_g$, latitude N – $\varphi_g$ (**Block 1**); upward radiance at the satellite level in spectral channels $\lambda_1$ – $L_u(\lambda_1)$, and $\lambda_2$ – $L_u(\lambda_2)$ (**Block 2**).

### Section B

**The model formulae are:**

**Block 3**

1. Geographical registration and geometric correction. Geographical registration was performed on the basis of information on the number of pixels and lines, the line scanning time (NOAA KLM 2005), and the model for predicting satellite position and velocity, SGP4 (Hoots & Roehrich 1988). The orbital parameters of the given satellite (inclination, eccentricity, ascending node, mean velocity etc.) were taken from the TLE (*Two-line element*) bulletin (http://celestrak.com/NORAD/elements/noaa.txt). The geographical position calculated in this way was then corrected according to the procedure put forward by Kowalewski & Krężel (2004). The geometric correction – the pixel brightness of exact grid centres after the geographical registration – was chosen using the nearest neighbourhood method.

**Block 4**

2. Brightness temperatures in channels 4 (10.3–11.3 $\mu$m) and 5 (11.5 –12.5 $\mu$m) of AVHRR are calculated according to a standard procedure that includes Planck's Law, the spectral response curves of channels, and the results of radiometer sensitivity calibration performed continuously on board of the satellite radiometer (http://www2.ncdc.noaa.gov/docs/klm/html/c7/sec7-1.htm).

**Block 5**

3. Sea surface temperature (NOAA KLM 2005):

$$NLSST = b_1 T4 + b_2(T4 - T5)\, MCSST + \\ + b_3(T4 - T5)(\sec\, \theta_{sat} - 1) + b_4, \tag{AII.1}$$

where

$$MCSST = a_1 T4 + a_2(T4 - T5) + a_3(T4 - T5)\times$$
$$\times(\sec\,\theta_{sat} - 1) + a_4, \qquad \text{(AII.2)}$$

$T4$ and $T5$ – respective brightness temperatures in AVHRR channels 4 and 5, $\theta_{sat}$ – zenith angle of the satellite, $a_n$, $b_n$ – empirical coefficients appropriate to the relevant satellite and time of day (night, day; Tab. AII.1).

**Section C**

**The principles of the computations are:**

Using the input data: Greenwich Mean Time – $GMT$, longitude E – $\lambda_g$, latitude N – $\varphi_g$ (**Block 1**); upward radiance at the satellite level in spectral channels $\lambda_1$ – $L_u(\lambda_1)$, and $\lambda_2$ – $L_u(\lambda_2)$ (**Block 2**) and the model formulae: (**Block 3**) satellite positioning formulae and the procedures enabling the geometric correction of the image and the precise geographical location (latitude and longitude $\varphi_g$ and $\lambda_g$) of each pixel (**Block 3**); formulae for the instrumental correction and definition of the brightness temperature in AVHRR channels 4 and 5 (**Block 4**); formulae for defining the sea surface temperature on the basis of AVHRR data (**Block 5**), the following parameters are calculated in turn: sea surface brightness temperature in AVHRR channels 4 ($T4$) and 5 ($T5$) (**Block 6**), and then the sea surface temperature $SST$ (**Block 7**).

**Table AII.1.** Coefficients of equations (1) and (2) for particular satellites and time of day (AVHRR 2002)

| MCSST Algorithm | | | | | |
|---|---|---|---|---|---|
| Satellite | Time | Coefficients | | | |
| | | $a_1$ | $a_2$ | $a_3$ | $a_4$ |
| NOAA-12 | day | 0.963563 | 2.579211 | 0.242598 | −263.006 |
| NOAA-12 | night | 0.967077 | 2.384376 | 0.480788 | −263.940 |
| NOAA-14 | day | 1.017342 | 2.139588 | 0.779706 | −278.430 |
| NOAA-14 | night | 1.029088 | 2.275385 | 0.752567 | −282.240 |
| NOAA-15 | day | 0.964243 | 2.712960 | 0.387491 | −262.443 |
| NOAA-15 | night | 0.976789 | 2.770720 | 0.435832 | −266.290 |
| NOAA-16 | day | 0.999314 | 2.301950 | 0.628976 | −273.768 |
| NOAA-16 | night | 0.995103 | 2.536570 | 0.753281 | −273.146 |
| NOAA-17 | day | 0.992818 | 2.499160 | 0.915103 | −271.206 |
| NOAA-17 | night | 1.010150 | 2.581500 | 1.000540 | −276.590 |

**Table AII.1.** (*continued*)

| NLSST Algorithm | | | | | |
|---|---|---|---|---|---|
| Satellite | Time | Coefficients | | | |
| | | $b_1$ | $b_2$ | $b_3$ | $b_4$ |
| NOAA-12 | day | 0.876992 | 0.083132 | 0.349877 | −236.667 |
| NOAA-12 | night | 0.888706 | 0.081646 | 0.576136 | −240.229 |
| NOAA-14 | day | 0.939813 | 0.076060 | 0.801458 | −255.165 |
| NOAA-14 | night | 0.933109 | 0.078095 | 0.738128 | −253.428 |
| NOAA-15 | day | 0.913116 | 0.090576 | 0.476940 | −246.887 |
| NOAA-15 | night | 0.922560 | 0.093611 | 0.548055 | −249.819 |
| NOAA-16 | day | 0.914471 | 0.077612 | 0.668532 | −248.116 |
| NOAA-16 | night | 0.898887 | 0.083933 | 0.755283 | −244.006 |
| NOAA-17 | day | 0.936047 | 0.083867 | 0.920848 | −253.951 |
| NOAA-17 | night | 0.938875 | 0.086427 | 0.979108 | −255.023 |

## Annex III. Mathematical apparatus of the subalgorithm for estimating the chlorophyll *a* concentration in the Baltic Sea surface layer

### Section A

**The input parameters are:**

- $TOA(\lambda_i)$ – satellite-measured upwelling radiance (**Block 1**). It is often described as the water-leaving radiance at the top of the atmosphere. The satellite-measured sensor data include the strong influence of the atmosphere on the measured upwelling radiance. This effect is later removed during the atmospheric corrections.

  Alternatively, the already corrected Remotely Sensed Reflectances $R_{rs}(\lambda)$ can be used as input data. In this case, **Block 3** is omitted. The equations in section B apply to the two ocean colour satellite sensors (SeaWiFS and MODIS) that are used the most at the present moment.

- Ancillary data, which are later utilised mainly in the atmospheric corrections (**Block 2**). These data include meteorological data from NCEP and TOMS/TOAST Ozone data. Both ancillary data sets are adapted to the atmospheric correction calculated in the Seadas software and widely available, e.g. http://oceancolor.gsfc.nasa.gov/ftp.html

**Section B**

**The models and algorithms are:**

**Block 3:** Atmospheric correction. Any suitable one for this type of water algorithm can be applied here. In the present work, the authors used the atmospheric correction scheme proposed by Ruddick et al. (2000), which has been proved to be the most suitable for the optically complex Baltic waters, but it is very likely that in the future new algorithms will be developed which will provide better results. In that case the new algorithms should be applied here.

**Block 4:** Chlorophyll *a* concentration in the surface layer $C_a(0)$. The form of the equations enabling the chlorophyll *a* concentration in the surface layer of water to be calculated on the basis of the atmospherically corrected upward radiation depends on the source of the satellite data. The equations adapted to the two most commonly used satellite scanners (SeaWiFs and MODIS) are given below.

- SeaWiFS algorithm ($SW$):

$$C_a(0) = 10^{1.311-0.7874XR-0.4935XR^2}, \tag{AIII.1}$$

where

$$XR = XR_{(SW)} = \frac{R_{rs}(510\text{ nm}) - R_{rs}(665\text{ nm})}{R_{rs}(555\text{ nm}) - R_{rs}(665\text{ nm})}, \tag{AIII.2}$$

$C_a(0)$ [mg m$^{-3}$] – surface layer concentration of chlorophyll *a*,

$R_{rs}(\lambda)$ [sr$^{-1}$] – remote sensing reflectance for wavelength $\lambda$,

$\lambda_i = 510$, 555, 675 nm.

- MODIS algorithm ($MD$):

$$C_a(0) = 10^{1.102-0.8708XR-0.3449XR^2}, \tag{AIII.3}$$

where

$$XR = XR_{(MD)} = \frac{R_{rs}(490\text{ nm}) - R_{rs}(665\text{ nm})}{R_{rs}(550\text{ nm}) - R_{rs}(665\text{ nm})}, \tag{AIII.4}$$

$\lambda_i = 490$, 550, 675 nm.

These two algorithms utilise satellite data where the surface reflectance (contribution due to 'white'-capping and Sun Glint, the direct + diffuse reflectance of the solar radiance from the sea surface)

is taken into account during the atmospheric correction (which is the usual approach at the moment). For the other cases, where the surface reflectance is not taken into account during the atmospheric correction, we propose new $XR$ coefficients that include corrections for the sky surface reflectance in simplified relationships:

- SeaWiFS algorithm ($SW$):
see eq. (AIII.1) where

$$XR = XR_{(SW)} = \frac{R_{rst}(510 \text{ nm}) - R_{rst}(665 \text{ nm}) - SF1_{(SW)}}{R_{rst}(555 \text{ nm}) - R_{rst}(665 \text{ nm}) - SF2}. \tag{AIII.5}$$

- MODIS algorithm ($MD$):
see eq. (AIII.3) where

$$XR = XR_{(MD)} = \frac{R_{rst}(490 \text{ nm}) - R_{rst}(665 \text{ nm}) - SF1_{(MD)}}{R_{rst}(550 \text{ nm}) - R_{rst}(665 \text{ nm}) - SF2}, \tag{AIII.6}$$

where $R_{rst}(\lambda)$ – total (diffuse and reflected) remote sensing reflectance; and the coefficients are introduced as:

$$SF1_{(SW)} =< R_{sf}(510) - R_{sf}(665) >, \tag{AIII.7}$$

$$SF1_{(MD)} =< R_{sf}(490) - R_{sf}(665) >, \tag{AIII.8}$$

$$SF2 =< R_{sf}(550) - R_{sf}(665) > . \tag{AIII.9}$$

$R_{sf}(\lambda)$ is the reflectance produced by surface reflection and is defined as:

$$R_{sf}(\lambda) = L_{us}(\lambda)/E_d(\lambda), \tag{AIII.10}$$

where
$L_{us}(\lambda)$ – the upward radiance reflected at the surface,
$E_d(\lambda)$ – downwelling irradiance above the sea surface.

Based on the number of measurements over the Baltic Sea for cloudless sky conditions, the approximate values of the above coefficients are proposed as follows:

For SeaWiFS data: $SF1_{SW} = 2.917 \times 10^{-4}$
For MODIS data: $SF1_{MD} = 6.8095 \times 10^{-4}$
For SeaWiFS and MODIS data: $SF2 = 5.5135 \times 10^{-5}$
(for more details, see Darecki et al. – in preparation).

**Section C**

**The principles of the calculations are:**

**Block 5:** the values of the remote sensing reflectance $R_{rs}(\lambda_i)$ for the relevant spectral channels are calculated with the aid of the atmospheric correction algorithms (implemented in the Seadas programme) defined in Block 3.

**Block 6:** surface layer concentrations of chlorophyll $a$ $C_a(0)$ are calculated using equations (AIII.1)–(AIII.6) adapted to the relevant satellite scanner.

## Annex IV. Mathematical apparatus of the subalgorithm for calculating the daily dose of PAR transmitted across a wind-blown sea surface

The mathematical apparatus presented below follows the consecutive blocks of the diagram presented in Figure 4.

**Section A**

The **input parameters** of the model are: average wind speed $v$ (wind speed measured 10 m above the sea surface and averaged for the particular day) (**Block 1**); latitude $\varphi_g$ and day of the year $DOY$ (**Block 2**); direct and diffuse components of the daily PAR dose just above the sea surface: $\eta_{PAR,dir}(0^+)$ and $\eta_{PAR,dif}(0^+)$.

**Section B**

**The model formulae are:**

**Block 4:** formula for the transmission coefficient of the direct component of the daily PAR dose (S. B. Woźniak – in preparation):

$$T_{\eta PAR,dir} = 1 - \left[ \left(1 - s_{foam}\right) \frac{\int\limits_{t_{\otimes sr}}^{t_{\otimes ss}} \cos(\theta_{\otimes}) R_d^{dir}(\theta_{\otimes}, v) dt}{\int\limits_{t_{\otimes sr}}^{t_{\otimes ss}} \cos(\theta_{\otimes}) dt} + s_{foam} A_{foam} \right], \tag{AIV.1}$$

where

– the cosine of the solar zenith angle can be calculated using the following set of formulae:

$$\cos(\theta_{\otimes}) = \sin\varphi_g \sin\delta_{\otimes} + \cos\varphi_g \cos\delta_{\otimes} \cos(\pi(15t_{\otimes} - 180)/180),$$

where

$$\delta_{\otimes} = 0.006918 - 0.399912\cos\psi + 0.070257\sin\psi - 0.006758 \times$$
$$\times \cos 2\psi + 0.000907 \sin 2\psi - 0.002697 \cos 3\psi + 0.00148 \sin 3\psi,$$

$$\psi = 2\pi(DOY - 1)/365$$

and $t_{\otimes}$ represents local time;

– the functional dependence of the irradiance reflectance with direct light on the solar zenith angle and wind speed $R_d^{dir}(\theta_{\otimes}, v)$ is given in the form of a look-up table (Table AIV.1);

– $t_{\otimes sr}$ and $t_{\otimes ss}$ stand for local sunrise and sunset times respectively;

– the fraction of the sea surface covered by foam is given by the formula (Monahan & O'Muircheartaigh 1986) $s_{foam} = 2.95 \times 10^{-6}\ v^{3.52}$;

– the albedo of the sea foam is assumed to be $A_{foam} = 0.22$ (Koepke 1984).

**Block 5:** formula for the transmission coefficient of the diffuse component of the daily PAR dose (S. B. Woźniak – in preparation):

$$T_{\eta PAR,dif} = 1 - \Big[(1 - s_{foam}) R_d^{dif}(v) + s_{foam} A_{foam}\Big], \tag{AIV.2}$$

where the functional dependence of irradiance reflectance with diffuse light on the wind speed $R_d^{dif}(v)$ is given in the form of a look-up table (Table AIV.2).

---

**Section C**

**The principles of the computations are:**

**Block 6:** the direct component of the daily PAR dose just below the sea surface can be calculated as

$$\eta_{PAR,dir}(0^-) = T_{\eta PAR,dir}\, \eta_{PAR,dir}(0^+). \tag{AIV.3}$$

**Block 7:** the diffuse component of the daily PAR dose just below the sea surface can be calculated as

$$\eta_{PAR,dif}(0^-) = T_{\eta PAR,dif}\, \eta_{PAR,dif}(0^+). \tag{AIV.4}$$

**Block 8:** the final value of the daily PAR dose transmitted across a wind-blown sea surface can be calculated as the following sum:

$$\eta_{PAR}(0^-) = \eta_{PAR,dir}(0^-) + \eta_{PAR,dif}(0^-). \tag{AIV.5}$$

**Table AIV.1.** Values of the irradiance reflectance with direct light $R_d^{dir}$ for different solar zenith angles and different wind speeds

| $\theta_\otimes$ [°] | $v =$ 1 m s$^{-1}$ | $v =$ 2 m s$^{-1}$ | $v =$ 3 m s$^{-1}$ | $v =$ 4 m s$^{-1}$ | $v =$ 5 m s$^{-1}$ | $v =$ 6 m s$^{-1}$ | $v =$ 7 m s$^{-1}$ | $v =$ 8 m s$^{-1}$ |
|---|---|---|---|---|---|---|---|---|
| 0 | 0.02114 | 0.02102 | 0.02091 | 0.02080 | 0.02069 | 0.02058 | 0.02047 | 0.02036 |
| 2.5 | 0.02114 | 0.02103 | 0.02092 | 0.02081 | 0.02070 | 0.02059 | 0.02048 | 0.02037 |
| 5 | 0.02114 | 0.02103 | 0.02092 | 0.02081 | 0.02071 | 0.02060 | 0.02050 | 0.02039 |
| 7.5 | 0.02115 | 0.02104 | 0.02093 | 0.02083 | 0.02073 | 0.02062 | 0.02052 | 0.02042 |
| 10 | 0.02116 | 0.02106 | 0.02095 | 0.02085 | 0.02075 | 0.02066 | 0.02056 | 0.02046 |
| 12.5 | 0.02118 | 0.02108 | 0.02099 | 0.02089 | 0.02080 | 0.02070 | 0.02061 | 0.02052 |
| 15 | 0.02122 | 0.02113 | 0.02104 | 0.02095 | 0.02086 | 0.02077 | 0.02068 | 0.02060 |
| 17.5 | 0.02128 | 0.02120 | 0.02111 | 0.02103 | 0.02095 | 0.02087 | 0.02079 | 0.02071 |
| 20 | 0.02138 | 0.02130 | 0.02122 | 0.02115 | 0.02108 | 0.02100 | 0.02093 | 0.02086 |
| 22.5 | 0.02152 | 0.02145 | 0.02138 | 0.02132 | 0.02125 | 0.02119 | 0.02112 | 0.02106 |
| 25 | 0.02171 | 0.02166 | 0.02160 | 0.02155 | 0.02150 | 0.02144 | 0.02139 | 0.02133 |
| 27.5 | 0.02199 | 0.02195 | 0.02191 | 0.02187 | 0.02183 | 0.02178 | 0.02174 | 0.02169 |
| 30 | 0.02237 | 0.02235 | 0.02232 | 0.02230 | 0.02227 | 0.02224 | 0.02221 | 0.02217 |
| 32.5 | 0.02289 | 0.02289 | 0.02288 | 0.02287 | 0.02286 | 0.02284 | 0.02282 | 0.02279 |
| 35 | 0.02358 | 0.02360 | 0.02361 | 0.02362 | 0.02363 | 0.02363 | 0.02362 | 0.02359 |
| 37.5 | 0.02450 | 0.02454 | 0.02458 | 0.02461 | 0.02464 | 0.02465 | 0.02465 | 0.02463 |
| 40 | 0.02571 | 0.02578 | 0.02585 | 0.02590 | 0.02595 | 0.02597 | 0.02598 | 0.02597 |
| 42.5 | 0.02729 | 0.02740 | 0.02749 | 0.02758 | 0.02764 | 0.02767 | 0.02768 | 0.02766 |
| 45 | 0.02935 | 0.02949 | 0.02962 | 0.02973 | 0.02980 | 0.02984 | 0.02984 | 0.02982 |
| 47.5 | 0.03201 | 0.03220 | 0.03237 | 0.03249 | 0.03257 | 0.03260 | 0.03258 | 0.03253 |
| 50 | 0.03546 | 0.03570 | 0.03590 | 0.03603 | 0.03609 | 0.03609 | 0.03604 | 0.03594 |
| 52.5 | 0.03991 | 0.04020 | 0.04041 | 0.04053 | 0.04055 | 0.04049 | 0.04037 | 0.04019 |
| 55 | 0.04565 | 0.04597 | 0.04617 | 0.04623 | 0.04617 | 0.04600 | 0.04577 | 0.04548 |
| 57.5 | 0.05304 | 0.05337 | 0.05350 | 0.05343 | 0.05321 | 0.05287 | 0.05246 | 0.05200 |
| 60 | 0.06253 | 0.06280 | 0.06277 | 0.06247 | 0.06198 | 0.06138 | 0.06071 | 0.06000 |
| 62.5 | 0.07473 | 0.07481 | 0.07443 | 0.07374 | 0.07284 | 0.07185 | 0.07080 | 0.06975 |
| 65 | 0.09036 | 0.08999 | 0.08901 | 0.08768 | 0.08617 | 0.08461 | 0.08306 | 0.08155 |
| 67.5 | 0.11031 | 0.10907 | 0.10707 | 0.10476 | 0.10238 | 0.10006 | 0.09784 | 0.09576 |
| 70 | 0.13564 | 0.13279 | 0.12919 | 0.12548 | 0.12193 | 0.11863 | 0.11560 | 0.11282 |
| 72.5 | 0.16748 | 0.16188 | 0.15592 | 0.15035 | 0.14534 | 0.14088 | 0.13690 | 0.13334 |
| 75 | 0.20702 | 0.19696 | 0.18784 | 0.18002 | 0.17335 | 0.16761 | 0.16263 | 0.15825 |
| 77.5 | 0.25590 | 0.23874 | 0.22582 | 0.21560 | 0.20727 | 0.20031 | 0.19438 | 0.18925 |
| 80 | 0.31920 | 0.28954 | 0.27212 | 0.25966 | 0.24997 | 0.24209 | 0.23548 | 0.22981 |
| 82.5 | 0.41487 | 0.35964 | 0.33526 | 0.32022 | 0.30945 | 0.30108 | 0.29424 | 0.28847 |
| 85 | 0.59988 | 0.48949 | 0.44926 | 0.42828 | 0.41511 | 0.40583 | 0.39877 | 0.39312 |
| 87.5 | 0.69489 | 0.56649 | 0.51694 | 0.49002 | 0.47271 | 0.46039 | 0.45101 | 0.44353 |
| 90 | 0.88298 | 0.69926 | 0.63231 | 0.59769 | 0.57640 | 0.56184 | 0.55116 | 0.54291 |

**Table AIV.1.** (*continued*)

| $\theta_{\otimes}$ [°] | $v =$ 9 m s$^{-1}$ | $v =$ 10 m s$^{-1}$ | $v =$ 11 m s$^{-1}$ | $v =$ 12 m s$^{-1}$ | $v =$ 13 m s$^{-1}$ | $v =$ 14 m s$^{-1}$ | $v =$ 15 m s$^{-1}$ |
|---|---|---|---|---|---|---|---|
| 0 | 0.02026 | 0.02015 | 0.02004 | 0.01994 | 0.01983 | 0.01972 | 0.01962 |
| 2.5 | 0.02027 | 0.02016 | 0.02006 | 0.01995 | 0.01985 | 0.01974 | 0.01964 |
| 5 | 0.02029 | 0.02019 | 0.02008 | 0.01998 | 0.01988 | 0.01978 | 0.01967 |
| 7.5 | 0.02032 | 0.02022 | 0.02012 | 0.02002 | 0.01992 | 0.01982 | 0.01972 |
| 10 | 0.02036 | 0.02027 | 0.02017 | 0.02008 | 0.01998 | 0.01988 | 0.01979 |
| 12.5 | 0.02043 | 0.02033 | 0.02024 | 0.02015 | 0.02006 | 0.01996 | 0.01987 |
| 15 | 0.02051 | 0.02042 | 0.02034 | 0.02025 | 0.02016 | 0.02007 | 0.01998 |
| 17.5 | 0.02063 | 0.02054 | 0.02046 | 0.02038 | 0.02029 | 0.02021 | 0.02012 |
| 20 | 0.02078 | 0.02071 | 0.02063 | 0.02055 | 0.02047 | 0.02039 | 0.02030 |
| 22.5 | 0.02099 | 0.02092 | 0.02085 | 0.02078 | 0.02070 | 0.02062 | 0.02054 |
| 25 | 0.02127 | 0.02121 | 0.02114 | 0.02107 | 0.02100 | 0.02092 | 0.02085 |
| 27.5 | 0.02164 | 0.02158 | 0.02152 | 0.02146 | 0.02139 | 0.02132 | 0.02124 |
| 30 | 0.02212 | 0.02207 | 0.02202 | 0.02195 | 0.02189 | 0.02182 | 0.02174 |
| 32.5 | 0.02275 | 0.02271 | 0.02265 | 0.02259 | 0.02253 | 0.02246 | 0.02238 |
| 35 | 0.02356 | 0.02352 | 0.02347 | 0.02341 | 0.02335 | 0.02327 | 0.02320 |
| 37.5 | 0.02461 | 0.02456 | 0.02451 | 0.02445 | 0.02438 | 0.02430 | 0.02422 |
| 40 | 0.02594 | 0.02589 | 0.02583 | 0.02577 | 0.02569 | 0.02560 | 0.02551 |
| 42.5 | 0.02763 | 0.02757 | 0.02750 | 0.02742 | 0.02733 | 0.02723 | 0.02712 |
| 45 | 0.02976 | 0.02969 | 0.02960 | 0.02950 | 0.02938 | 0.02926 | 0.02913 |
| 47.5 | 0.03245 | 0.03234 | 0.03222 | 0.03208 | 0.03193 | 0.03177 | 0.03160 |
| 50 | 0.03581 | 0.03565 | 0.03547 | 0.03528 | 0.03508 | 0.03487 | 0.03465 |
| 52.5 | 0.03999 | 0.03975 | 0.03949 | 0.03923 | 0.03895 | 0.03867 | 0.03839 |
| 55 | 0.04515 | 0.04480 | 0.04444 | 0.04406 | 0.04369 | 0.04331 | 0.04293 |
| 57.5 | 0.05151 | 0.05100 | 0.05048 | 0.04996 | 0.04945 | 0.04894 | 0.04845 |
| 60 | 0.05927 | 0.05854 | 0.05782 | 0.05712 | 0.05643 | 0.05576 | 0.05512 |
| 62.5 | 0.06871 | 0.06769 | 0.06671 | 0.06576 | 0.06485 | 0.06399 | 0.06316 |
| 65 | 0.08010 | 0.07872 | 0.07741 | 0.07617 | 0.07500 | 0.07389 | 0.07284 |
| 67.5 | 0.09381 | 0.09199 | 0.09029 | 0.08870 | 0.08722 | 0.08583 | 0.08453 |
| 70 | 0.11028 | 0.10749 | 0.10579 | 0.10381 | 0.10198 | 0.10028 | 0.09869 |
| 72.5 | 0.13013 | 0.12723 | 0.12460 | 0.12219 | 0.11998 | 0.11795 | 0.11606 |
| 75 | 0.15437 | 0.15089 | 0.14777 | 0.14493 | 0.14234 | 0.13997 | 0.13778 |
| 77.5 | 0.18474 | 0.18075 | 0.17718 | 0.17395 | 0.17103 | 0.16835 | 0.16589 |
| 80 | 0.22488 | 0.22052 | 0.21664 | 0.21315 | 0.20998 | 0.20709 | 0.20444 |
| 82.5 | 0.28348 | 0.27909 | 0.27519 | 0.27167 | 0.26848 | 0.26557 | 0.26289 |
| 85 | 0.38840 | 0.38437 | 0.38083 | 0.37769 | 0.37486 | 0.37227 | 0.36991 |
| 87.5 | 0.43735 | 0.43212 | 0.42760 | 0.42363 | 0.42010 | 0.41693 | 0.41406 |
| 90 | 0.53630 | 0.53083 | 0.52620 | 0.52222 | 0.51874 | 0.51565 | 0.51289 |

**Table AIV.2.** Values of the irradiance reflectance with diffuse light $R_d^{dif}$ for different wind speeds (for the case of cardioidal diffuse sky radiance distribution in which radiance is proportional to the following term: $(1 + 2\cos(\theta))$

| Wind speed $v$ [m s$^{-1}$] | 1 | 2 | 3 | 4 | 5 | 6 | 7 | 8 |
|---|---|---|---|---|---|---|---|---|
| Reflectance $R_d^{dif}$ | 0.05477 | 0.05196 | 0.05047 | 0.04941 | 0.04853 | 0.04777 | 0.04708 | 0.04645 |
| Wind speed $v$ [m s$^{-1}$] | 9 | 10 | 11 | 12 | 13 | 14 | 15 | |
| Reflectance $R_d^{dif}$ | 0.04585 | 0.04528 | 0.04475 | 0.04423 | 0.04373 | 0.04326 | 0.04279 | |

## Annex V. Mathematical apparatus of the subalgorithm for estimating the underwater optical and bio-optical features and photosynthetic primary production in the Baltic Sea

The mathematical apparatus of the general model of marine primary production with all its component bio-optical relationships is given here as a kind of algorithm. It follows the consecutive blocks of the diagram presented in Figure 6 of this paper. The algorithm has been developed for the practical remote sensing of the bio-optical properties of the sea.

### Section A

The **input parameters** of the model are the surface chlorophyll concentration $C_a(0)$ [mg tot. chl $a$ m$^{-3}$] (**Block 1**), the surface downward irradiance $PAR(0^-)$ [Ein m$^{-2}$ s$^{-1}$] or scalar irradiance $PAR_0(0^-)$ [Ein m$^{-2}$ s$^{-1}$] (**Block 2**), and the sea surface temperature *temp* [°C] (**Block 3**).

### Section B

### The model formulae are:

**Block 4:** relationships between the vertical profiles in Baltic waters of the chlorophyll $a$ concentration $C_a(z)$ and its surface concentration $C_a(0)$ (Ostrowska et al. 2007):

$$C_a(z) = C_a(0)\frac{A + B\exp[-(z - z_m)^2 \times \sigma]}{A + B\exp[-(z_m)^2 \times \sigma]}, \tag{AV.1}$$

where

$A = 10^{(1.38\log(C_a(0))+0.0883)}$, $B = 10^{(0.714\log(C_a(0))+0.0233)}$,

$z_m = -4.61\log(C_a(0)) + 8.86)$, $\sigma = 0.0052$.

**Block 5:** bio-optical relationships for estimating the following optical quantities (Woźniak et al. 1992a,b, 1995, Woźniak & Olszewski 1995, Kaczmarek & Woźniak 1995):

- optical depth in the sea

$$\tau(z) = -\ln T(z); \tag{AV.2}$$

- downward irradiance spectral distribution functions

$$f_E(\lambda, z) = f_E(\lambda, 0) \exp\left[-\int_0^z K_d(\lambda, z) dz\right]; \tag{AV.3}$$

- transmittance of irradiance through the water column

$$T(z) = \int_{400\,\mathrm{nm}}^{700\,\mathrm{nm}} f_E(\lambda, z) d\lambda; \tag{AV.4}$$

- downward spectral irradiance

$$E_d(\lambda, z) = PAR(0^+) f_E(\lambda, z); \tag{AV.5}$$

- overall irradiances in the PAR range
  (downward vectors)

$$PAR(z) = PAR(0^-) T(z), \tag{AV.6a}$$

  (scalar)

$$PAR(z) \approx 1.2 PAR(0^-) T(z), \tag{AV.6b}$$

  where

  $K_d(\lambda, z)$ – downward spectral irradiance diffuse attenuation coefficient,

  $f_E(\lambda, 0)$ – normalised typical spectral distribution of PAR irradiance entering the sea (see Woźniak & Hapter 1985, Dera 1995) $\int_{400\,\mathrm{nm}}^{700\,\mathrm{nm}} f_E(\lambda, 0) d\lambda = 1$.

  The function $f_E(\lambda, 0)$ is described by the approximate polynomial expression:

$$\begin{aligned} f_E(\lambda, 0) = {} & -1.3702 \times 10^{-12} \lambda^4 + 3.4125 \times 10^{-9} \lambda^3 - 3.1427 \times \\ & \times 10^{-6} \lambda^2 + 1.2647 \times 10^{-3} \lambda - 1.8381 \times 10^{-1}, \end{aligned} \tag{AV.7}$$

  where $\lambda$ is expressed in [nm].

The coefficient $K_d(\lambda, z)$ is related to the chlorophyll concentration $C_a(z)$:

$$K_d(\lambda, z) = K_w(\lambda) + C_a(z)\{c_1(\lambda)\exp[-a_1(\lambda)C_a(z)] + k_{d,i}(\lambda)\} + \Delta K(\lambda), \quad \text{(AV.8)}$$

where $\Delta K(\lambda)$ for Baltic case 2 waters is (Kaczmarek & Woźniak 1995):

$$\Delta K(\lambda) = 0.068 \times \exp[-0.014(\lambda - 550)].$$

The constants $c_1(\lambda)$, $a_1(\lambda)$, $k_{d,i}(\lambda)$ and the attenuation of pure water $K_w(\lambda)$ are given in Table AV.1.

**Block 6:** relationships for estimating the vertical profiles of pigment concentrations in the Baltic (Majchrowski et al. 2007):

- for photosynthetic pigments:

  winter

$$C_{PSC} = C_a \times 10^{-1.436+0.064027\tau-0.0054346\tau^2+0.29550x-0.0065549x\tau+0.015895x^2} \quad \text{(AV.9a)}$$

  summer

$$C_{PSC} = C_a \times 10^{-0.82451+0.072685\tau-0.014871\tau^2+0.016015x+0.010256x\tau+0.029283x^2} \quad \text{(AV.9b)}$$

  winter

$$C_b = C_a \times 10^{-1.0703-0.15999\tau+0.046312\tau^2-0.30871x-0.040076x\tau-0.074687x^2} \quad \text{(AV.10a)}$$

  summer

$$C_b = C_a \times 10^{-0.8808+0.075078\tau-0.023728\tau^2-0.54886x+0.046307x\tau+0.20785x^2} \quad \text{(AV.10b)}$$

  winter

$$C_c = C_a \times 10^{-1.2314+0.14836\tau-0.031219\tau^2+0.051019x-0.0093837x\tau+0.053311x^2} \quad \text{(AV.11a)}$$

  summer

$$C_c = C_a \times 10^{-1.1330+0.1146\tau-0.020600\tau^2-0.011478x+0.0037213x\tau-0.0082814x^2} \quad \text{(AV.11b)}$$

winter

$$C_{phyc} = C_a \times 10^{1.0366-0.15103\tau+0.0280991\tau^2-0.53620x+0.039989x\tau+0.15519x^2} \tag{AV.12a}$$

summer

$$C_{phyc} = C_a \times 10^{1.0855-0.059569\tau+0.0022592\tau^2-0.63758x+0.068297x\tau+0.26215x^2} \tag{AV.12b}$$

- for photoprotecting carotenoids:

$$C_{PPC}/C_a = 0.164 \times < PDR^* >_{\Delta z} + 0.164, \tag{AV.13}$$

where $C_b$, $C_c$, $C_{PSC}$, $C_{phyc}$, $C_{PPC}$ [mg pigment m$^{-3}$] – concentrations of chlorophylls *b*, chlorophylls *c*, photosynthetic carotenoids *PSC*, phycobilins *phyc* and photoprotecting carotenoids *PPC* respectively,

$x = \log(C_a(0))$,

$\tau$ – optical depth, whose dependence on depth $z$ is described by the set of equations (AV.2)–(AV.8),

$< PDR^* >_{\Delta z}$ – mean values of the photo-adaptation factor in a water layer $\Delta z = z_2 - z_1$:

$$< PDR^* >_{\Delta z} = \frac{1}{z_2 - z_1} \int_{z_1}^{z_2} PDR^*(z) dz, \tag{AV.14}$$

where $z_2 = z + 15$ m and $z_1 = 0$ if $z < 15$ m or $z_1 = z + 15$ m if $z \geq 15$ m. The mean values in a water layer $\Delta z$ have been taken to include the influence of water mixing.

The Potentially Destructive Radiation (PDR) is defined as follows:

$$PDR^* = \int_{400\,\mathrm{nm}}^{480\,\mathrm{nm}} a_a^*(\lambda) < E_0(\lambda) >_{day} d\lambda, \tag{AV.15}$$

where

$PDR^*$ [$\mu$Ein (mg tot. chl *a*)$^{-1}$ s$^{-1}$] – the potentially destructive radiation per unit mass of chlorophyll *a* (the asterisk indicates that this is the $PDR$ per unit mass of chlorophyll *a*),

$E_0(\lambda)$ [$\mu$Ein m$^{-2}$ s$^{-1}$ nm$^{-1}$] – the scalar irradiance in the medium – $< E_0(\lambda) >_{day}$ stands for the mean daily value of this irradiance typical of a given season, region and depth in the sea,

$a_a^*(\lambda)$ [m$^2$(mg tot. chl $a$)$^{-1}$] – the specific coefficient of light absorption by chlorophyll $a$.

**Block 7:** Model relationships between different optical capacities of marine phytoplankton and pigment concentrations in the Baltic (Ficek et al. 2004):

- relationship between the product $C_I d$ and the chlorophyll concentration $C_a$ at depth $z$:

$$C_I d = 10.77 \times C_a^{0.3767}, \tag{AV.16}$$

where
$C_I$ [mg tot. chl $a$ m$^{-3}$] – intracellular chlorophyll $a$ concentration;
$d$ [m] – cell diameter, (value of $C_a$ given in [mg tot. chl $a$ m$^{-3}$]);

- relationships between the specific absorption coefficient of 'unpackaged' pigments (i.e. in solvent) and the chlorophyll $a$ concentration:

**(i)** for the j-th pigment group

$$a_j^*(\lambda) = \sum_i a^*_{\max,i} \times e^{-\frac{1}{2}\left(\frac{\lambda - \lambda_{\max,i}}{\sigma_i}\right)^2}, \tag{AV.17}$$

where
$\lambda_{\max,i}$ [nm] – centre of the spectral peak of the band,
$\sigma_i$ [nm] – dispersion of the band,
$a^*_{\max,i}$ [m$^2$(mg pigment)$^{-1}$] – specific absorption coefficient in the spectral peak of the band,
$i$ – Gaussian band numbers of major groups of phytoplankton pigments (e.g. chlorophylls $a$, chlorophylls $b$, chlorophylls $c$, photosynthetic carotenoids $PSC$, phycobilins $phyc$ and photoprotecting carotenoids $PPC$). The values of $\lambda_{\max,i}$, $\sigma_i$ and $a^*_{\max,i}$ are given in Table AV.2,

**(ii)** for photosynthetic pigments $PSC$ (in solvent – index S):

$$a^*_{PSP,S}(\lambda) = \frac{1}{C_a}\Big[C_a \times a_a^*(\lambda) + C_b \times a_b^*(\lambda) + C_c \times a_c^*(\lambda) + \\ + C_{PSC} \times a^*_{PSC}(\lambda) + C_{phyc} \times a^*_{phyc}(\lambda)\Big], \tag{AV.18}$$

**(iii)** for photoprotecting pigments $PPP$ (in solvent – index S):

$$a^*_{PPP,S}(\lambda) = \frac{1}{C_a}\Big[C_{PPC} \times a^*_{PPC}(\lambda)\Big], \tag{AV.19}$$

**(iv)** for all the phytoplankton pigments (in solvent – index S):

$$a^*_{pl,S}(\lambda) = a^*_{PSP,S}(\lambda) + a^*_{PPP,S}(\lambda); \tag{AV.20}$$

- the relationship between the package effect spectral function $Q^*(\lambda)$, the product $C_I \times d$ and the 'unpackaged' absorption coefficient $a^*_{pl,S}$ is:

$$Q^*(\lambda) = \frac{3}{2\rho'(\lambda)}\left[1 + \frac{2e^{-\rho'(\lambda)}}{\rho'(\lambda)} + 2\frac{e^{-\rho'(\lambda)} - 1}{\rho'^2(\lambda)}\right], \tag{AV.21}$$

where $\rho' = a^*_{pl,S} \times C_I \times d$ (the cell size optical parameter);

- the relationships between in vivo absorption coefficients, 'unpackaged' absorption coefficients (index S) and the package effect function:

**(i)** total for all phytoplankton pigments:

$$\left.\begin{aligned} a_{pl}(\lambda) &= C_a\, a^*_{pl}(\lambda) \\ a^*_{pl}(\lambda) &= Q^*(\lambda) a^*_{pl,S}(\lambda) \end{aligned}\right\} \tag{AV.22}$$

**(ii)** for photosynthetic pigments $PSP$ :

$$\left.\begin{aligned} a_{pl,PSP}(\lambda) &= C_a\, a^*_{pl,PSP}(\lambda) \\ a^*_{pl,PSP}(\lambda) &= Q^*(\lambda) a^*_{PSP,S}(\lambda) \end{aligned}\right\} \tag{AV.23}$$

**(iii)** for photoprotecting pigments:

$$\left.\begin{aligned} a_{pl,PPP}(\lambda) &= C_a\, a^*_{pl,PPP}(\lambda) \\ a^*_{pl,PPP}(\lambda) &= Q^*(\lambda) a^*_{PPP,S}(\lambda) \end{aligned}\right\} \tag{AV.24}$$

- these coefficients constitute the basis for determining the number of quanta of light absorbed by:

**(i)** all phytoplankton pigments:

$$PUR(z,t) = \int\limits_{400\,\mathrm{nm}}^{700\,\mathrm{nm}} E_0(\lambda, z, t) a_{pl}(\lambda, t) d\lambda, \tag{AV.25}$$

**(ii)** all phytoplankton pigments per unit mass of chlorophyll $a$:

$$\begin{aligned} PUR^*(z,t) &= \int\limits_{400\,\mathrm{nm}}^{700\,\mathrm{nm}} E_0(\lambda, z, t) a^*_{pl}(\lambda, t) d\lambda = \\ &= \tilde{a}^*_{pl}(z,t) PAR_0(z,t), \end{aligned} \tag{AV.26}$$

**(iii)** photosynthetic phytoplankton pigments:

$$PUR_{PSP}(z,t) = \int\limits_{400\,\mathrm{nm}}^{700\,\mathrm{nm}} E_0(\lambda,z,t)a_{pl,PSP}(\lambda,t)d\lambda, \quad \text{(AV.27)}$$

**(iv)** photosynthetic phytoplankton pigments per unit of chlorophyll $a$ mass:

$$\begin{aligned} PUR^*_{PSP}(z,t) &= \int\limits_{400\,\mathrm{nm}}^{700\,\mathrm{nm}} E_0(\lambda,z,t)a^*_{pl,PSP}(\lambda,t)d\lambda = \\ &= \tilde{a}^*_{pl,PSP}(z,t)PAR_0(z,t), \end{aligned} \quad \text{(AV.28)}$$

**(v)** daily quanta doses absorbed by phytoplankton:

$$\eta_{PUR}(z) = \int\limits_{t_{rise}}^{t_{set}} PUR(z,t)dt, \quad \text{(AV.29)}$$

$$\eta_{PUR,PSP}(z) = \int\limits_{t_{rise}}^{t_{set}} PUR_{PSP}(z,t)dt, \quad \text{(AV.30)}$$

where

$E_0(\lambda,z,t)$ – spectral scalar irradiance ($E_0 \approx 1.2\,E_d$),

$\tilde{a}^*_{pl}$ – mean specific absorption coefficient of phytoplankton, weighted by the irradiance spectrum,

$\tilde{a}^*_{pl,PSP}$ – mean specific absorption coefficient of photosynthetic pigments, weighted by the irradiance spectrum,

$t_{rise}$ – time of sunrise, $t_{set}$ – time of sunset.

**Block 8:** The model relationships between the quantum yield of photosynthesis and environmental parameters in the Baltic are as follows (Woźniak et al. 2007a,b):

$$\Phi = \Phi_{MAX}\, f_a\, f_\Delta\, f_{c(C_a(0))}\, f_{c(PARinh,temp)}\, f_{E,t}, \quad \text{(AV.31)}$$

where

$$\Phi_{MAX} = 0.125 \text{ atom C quanta}^{-1} \quad \text{(AV.32)}$$

(theoretical maximum quantum yield of photosynthesis);

- non-photosynthetic pigment factor:

$$f_a = \frac{\tilde{a}^*_{pl,PSP}}{\tilde{a}^*_{pl}} \text{ or } f_a = PUR^*_{PSP}/PUR^*; \tag{AV.33}$$

- inefficiency factor in energy transfer and charge recombination:

$$f_\Delta = 0.408; \tag{AV.34}$$

- the relative number of functioning reaction centres:

  – the factor describing the influence of water trophicity (i.e. the surface concentration of chlorophyll *a* $C_a(0)$) on the number of functioning centres:

$$f_{c(C_a(0))} = \frac{C_a(0)^{2.48}}{0.15 + C_a(0)^{2.48}} \tag{AV.35}$$

  (where $C_a(0)$ is given in [mg tot. chl *a* $\mathrm{m}^{-3}$]),

  – the factor describing the reduction in the portion of functional PS2 reaction centres as a result of photoinhibition:

$$f_{c(PARinh,temp)} = \exp\left(\frac{-4860746 \times PAR^2}{2.23^{0.1\,temp}}\right); \tag{AV.36}$$

- the classic dependence of photosynthesis on light and temperature, also known as the light curve of photosynthetic efficiency at a given temperature:

$$f_{E,t} = \left[1 - \exp\left(\frac{-PUR^*_{PSP}}{5.237 \times 10^{-7} \times 2.03^{0.1\,temp}}\right)\right] \times$$

$$\times \frac{5.237 \times 10^{-7} \times 2.03^{0.1\,temp}}{PUR^*_{PSP}}. \tag{AV.37}$$

## Section C:

**The principles of the computations are:**

**Block 9:** vertical profiles of chlorophyll $C_a(z)$ can be calculated from input data $C_a(0)$ using eq. (AV.1).

**Block 10:** vertical profiles of optical depth $\tau(z)$, the relative function of spectral distribution of downward irradiance $f_E(\lambda, z)$, the PAR irradiance transmittance $T(z)$, the diffuse attenuation coefficient of the downward spectral irradiance $K_d(\lambda, z)$ and vertical profiles of irradiances $E_d(\lambda, z)$, $PAR(z)$ (or $PAR_0(z)$) can be calculated from their relationships with $C_a(z)$ and $PAR(0^+)$ irradiance input data using eqs. (AV.2)–(AV.8).

**Block 11:** vertical profiles of the relative concentration of particular phytoplankton pigments $C_j/C_a$ can be determined from the optical properties of the sea and the vertical profiles of chlorophyll *a* concentrations using eqs. (AV.9)–(AV.15).

**Block 12:** vertical profiles of the marine phytoplankton total spectral absorption coefficient and its components, and of the number of quanta and daily quanta doses absorbed by phytoplankton, and also the vertical distribution of the package effect spectral function $Q^*(\lambda, z)$ can be determined from basic unpackaged absorption coefficients, the package effect function and chlorophyll concentrations using eqs. (AV.16)–(AV.30).

**Block 13:** vertical profiles of the quantum yield of photosynthesis $\Phi(z)$ can be determined from the surface concentration of chlorophyll *a* $C_a(0)$, the vertical $PAR$ distribution (eq. (AV.6a)), the number of quanta absorbed by phytoplankton $PUR^*$ and $PUR^*_{PSP}$ (eqs. (AV.26) and (AV.28)) and temperature input data using eqs. (AV.31)–(AV.37).

**Block 14:** the vertical distribution of the daily primary production $P(z)$ [gC m$^{-3}$] can be determined from the quantum yield of photosynthesis $\Phi(z)$ (eqs. (AV.31)–(AV.37)) and the dose of $\eta_{PUR}$ [Ein m$^{-3}$] (eq. (AV.29)) using the formal relationships:

$$P(z) = 12 \times \Phi(z)\eta_{PUR}(z). \tag{AV.38}$$

The total daily primary production in the water column $P_{tot}$ [gC m$^{-2}$] is determined by numerical integration over the depth of the profiles $P(z)$:

$$P_{tot} = \int_0^{z(P=0)} P(z)dz, \tag{AV.39}$$

where $z(P = 0)$ is the depth at which primary production falls to a level so small that it does not affect the overall production $P_{tot}$.

**Table AV.1.** Values of parameters in the bio-optical classification of seas used in model equation (AV.8) (after Woźniak et al. 1992a,b)

| $\lambda$ [nm] | $a_1$ [$m^3$(mg tot. chl $a$)$^{-1}$] | $c_1$ [$m^2$ (mg tot. chl $a$)$^{-1}$] | $K_{d,i}$ | $K_w$ [$m^{-1}$] |
|---|---|---|---|---|
| 400 | 0.441 | 0.141 | 0.0675 | 0.0209 |
| 410 | 0.495 | 0.137 | 0.0643 | 0.0197 |
| 420 | 0.531 | 0.131 | 0.0626 | 0.0187 |
| 430 | 0.580 | 0.119 | 0.0610 | 0.0177 |
| 440 | 0.619 | 0.111 | 0.0609 | 0.0176 |
| 450 | 0.550 | 0.107 | 0.0569 | 0.0181 |
| 460 | 0.487 | 0.0950 | 0.0536 | 0.0189 |
| 470 | 0.500 | 0.0970 | 0.0479 | 0.0198 |
| 480 | 0.500 | 0.0780 | 0.0462 | 0.0205 |
| 490 | 0.509 | 0.0774 | 0.0427 | 0.0230 |
| 500 | 0.610 | 0.0672 | 0.0389 | 0.0276 |
| 510 | 0.594 | 0.0598 | 0.0363 | 0.0371 |
| 520 | 0.590 | 0.0610 | 0.0319 | 0.0473 |
| 530 | 0.693 | 0.0573 | 0.0288 | 0.0513 |
| 540 | 0.606 | 0.0506 | 0.0285 | 0.0567 |
| 550 | 0.514 | 0.0432 | 0.0274 | 0.0640 |
| 560 | 0.465 | 0.0425 | 0.0248 | 0.0720 |
| 570 | 0.384 | 0.0288 | 0.0240 | 0.0810 |
| 580 | 0.399 | 0.0230 | 0.0231 | 0.107 |
| 590 | 0.365 | 0.0180 | 0.0231 | 0.143 |
| 600 | 0.333 | 0.0171 | 0.0225 | 0.212 |
| 610 | 0.304 | 0.0159 | 0.0216 | 0.236 |
| 620 | 0.316 | 0.0150 | 0.0225 | 0.264 |
| 630 | 0.421 | 0.0183 | 0.0225 | 0.295 |
| 640 | 0.420 | 0.0216 | 0.0226 | 0.325 |
| 650 | 0.346 | 0.0164 | 0.0236 | 0.343 |
| 660 | 0.348 | 0.0141 | 0.0260 | 0.393 |
| 670 | 0.173 | 0.00939 | 0.0267 | 0.437 |
| 675 | 0.173 | 0.00436 | 0.0270 | 0.455 |
| 680 | 0.173 | 0 | 0.0258 | 0.478 |
| 690 | | 0 | 0.0190 | 0.535 |
| 700 | | 0 | 0.0125 | 0.626 |
| 710 | | 0 | 0.0045 | 1.000 |
| 720 | | 0 | 0.0014 | 1.360 |
| 730 | | 0 | 0.00041 | 1.810 |
| 740 | | 0 | $7.1\ 10^{-5}$ | 2.393 |
| 750 | | 0 | $1.3\ 10^{-5}$ | 2.990 |

**Table AV.2.** Model properties of the specific absorption components of Gaussian bands for Baltic phytoplankton pigments (after Ficek et al. 2004)

Chlorophylls *a*

| Property | Gaussian band number | | | | | |
|---|---|---|---|---|---|---|
| | A-1 | A-2 | A-3 | A-4 | A-5 | A-6 |
| $\lambda_{\max,i}$ | 381 | 418 | 439 | 635 | 676 | 708 |
| $\sigma_i$ | 37.7 | 10.0 | 9.72 | 29.9 | 10.7 | 14.4 |
| $a^*_{\max,i}$ | 0.0296 | 0.0151 | 0.0238 | 0.0067 | 0.0210 | 0.0008 |

Chlorophylls *b*

| Property | Gaussian band number | | | | | |
|---|---|---|---|---|---|---|
| | B-1 | B-2 | B-3 | B-4 | B-5 | B-6 |
| $\lambda_{\max,i}$ | 380 | 442 | 452 | 470 | 609 | 655 |
| $\sigma_i$ | 194 | 7.45 | 5.6 | 10.5 | 16.0 | 18.5 |
| $a^*_{\max,i}$ | 0.0059 | 0.0145 | 0.0631 | 0.0514 | 0.0083 | 0.0257 |

Chlorophylls *c*

| Property | Gaussian band number | | | | |
|---|---|---|---|---|---|
| | C-1 | C-2 | C-3 | C-4 | C-5 |
| $\lambda_{\max,i}$ | 408 | 432 | 460 | 583 | 640 |
| $\sigma_i$ | 16.1 | 7.93 | 14.2 | 16.0 | 16.0 |
| $a^*_{\max,i}$ | 0.0561 | 0.0234 | 0.0720 | 0.0073 | 0.0060 |

Photosynthetic carotenoids

| Property | Gaussian band number | | | |
|---|---|---|---|---|
| | PSC-1 | PSC-2 | PSC-3 | PSC-4 |
| $\lambda_{\max,i}$ | 468 | 490 | 515 | 532 |
| $\sigma_i$ | 26.7 | 17.1 | 13.1 | 22.8 |
| $a^*_{\max,i}$ | 0.0311 | 0.0313 | 0.0096 | 0.0194 |

Photoprotecting carotenoids

| Property | Gaussian band number | | |
|---|---|---|---|
| | PPC-1 | PPC-2 | PPC-3 |
| $\lambda_{\max,i}$ | 438 | 465 | 492 |
| $\sigma_i$ | 29.7 | 9.24 | 11.7 |
| $a^*_{\max,i}$ | 0.0516 | 0.0622 | 0.0560 |

Phycobilins

| Property | Gaussian band number | |
|---|---|---|
| | Phyc 1 | Phyc 2 |
| $\lambda_{\max,i}$ | 502 | 557 |
| $\sigma_i$ | 33.2 | 31.2 |
| $a^*_{\max,i}$ | 0.0015 | 0.0013 |

where $\lambda_{\max,i}$ – band centre [nm], $\sigma_i$ – band dispersion, $a^*_{\max,i}$ – specific absorption coefficient at the maximum [$m^2$ (mg pigment)$^{-1}$].